NRL Report 6137

Metallurgical Characteristics of High Strength Structural Materials

(FOURTH QUARTERLY REPORT)

R. J. Goode, R. W. Huber, D. G. Howe, R. W. Judy, T. W. Crooker,
R. E. Morey, E. A. Lange, P. P. Puzak, and K. B. Lloyd

Metallurgy Division

June 1964

U.S. NAVAL RESEARCH LABORATORY
Washington, D.C.

PREVIOUS REPORTS IN THIS SERIES

"Metallurgical Characteristics of High Strength Structural Materials (First Quarterly Report)," Puzak, Lloyd, Lange, Goode, Huber, Dahlberg, and Beachem, NRL Memorandum Report 1438, June 1963

"Metallurgical Characteristics of High Strength Structural Materials (Second Quarterly Report)," Puzak, Lloyd, Lange, Goode, and Huber, NRL Memorandum Report 1461, Sept. 1963

"Metallurgical Characteristics of High Strength Structural Materials (Third Quarterly Report)," Puzak, Lloyd, Goode, Huber, Howe, Crooker, and Lange, NRL Report 6086, Jan. 1964

Copies available at Office of Technical Services
Department of Commerce - $1.50

CONTENTS

ABSTRACT

A progress report covering research studies in high-strength hull structural materials, conducted in the period February 1964 to April 1964, is presented. These studies included the development of preliminary relationships of flaw size and stress for fracture of quenched and tempered steels, maraging steels, and titanium. Preliminary information was developed on the relationships of fracture toughness tests for aluminum. Heat-treatment studies for titanium alloys indicated improvements in fracture toughness for specific levels of yield strength. Evidence that low-cycle fatigue crack growth is a strain-controlled process is presented for specially rolled and heat treated HY-80 steels.

PROBLEM STATUS

This is a progress report; work is continuing.

AUTHORIZATION

NRL Problem M03-01
Projects SR 007-01-01-0850 and SR 007-01-01-0854

NRL Problem M01-18
Project SR 007-01-01-0856

NRL Problem M01-05
Project SR 007-01-02-0704

Manuscript submitted June 22, 1964.

METALLURGICAL CHARACTERISTICS

OF HIGH STRENGTH STRUCTURAL MATERIALS

(Fourth Quarterly Report)

INTRODUCTION

This is the fourth status report covering the U.S. Naval Research Laboratory's long-range program of determining the performance characteristics of high strength materials. Presently under investigation are quenched and tempered (Q&T) steels, maraging steels, titanium alloys, and aluminum alloys.

Flaw size-stress level requirements for fracture are presented for high strength titanium alloys. Additional explosion tear tests (ETT) for these requirements have undergone some modification from those reported earlier (1). ETT results for plates without flaws and with 2-in. flaws are reported for 3-5% strain deformations. The additional ETT data has resulted in a refinement of the preliminary correlations reported earlier (1) of ETT with drop-weight tear test (DWTT), Charpy V-notch, and yield strength (YS). ETT and DWTT correlations on the original Ti-8Al-2Cb-1Ta alloy plate material and two Ti-7Al-2Cb-1Ta alloys are presented. Results of the study on optimizing the strength and toughness properties for several of the more promising titanium alloys are reported.

Small laboratory tests (tensile, Charpy V, and DWTT) were conducted on five aluminum alloys representing a range of strength and toughness levels. The results of these studies indicate that the DWTT shows promise for indicating distinct differences in fracture toughness information of aluminum alloys. Preliminary correlations between YS, C_V, and DWTT are presented.

Further insight on the effect of strain in low-cycle fatigue crack growth has been obtained from the results of two series of tests on specially rolled and heat treated HY-80 steels. The first series of tests indicate the existence of a value of total strain range below which fatigue cracks cease to propagate at a rate which would result in a terminal failure from less than 100,000 load cycles. The second series of tests shows that the introduction of prestrain or positive mean strain can triple the crack growth rates, thereby decreasing low-cycle fatigue life.

EVALUATION OF TITANIUM ALLOYS

FOR DEEP-DIVING SUBMARINE HULL APPLICATIONS

(R. J. Goode, R. W. Huber, and D. G. Howe)

The tensile and fracture toughness properties of a variety of hot-rolled and heat-treated titanium alloy 1-inch-thick plates are being investigated. The major interest in these studies is the attainment of the ability to predict the fracture resistance of these materials in the presence of flaws (as indicated by the explosion tear test (ETT)) from the results obtained from laboratory tests such as the Charpy V (C_V) and drop-weight tear tests (DWTT). Preliminary correlations between the yield strength (YS), C_V, ETT, and DWTT were presented in a previous issue (1). Additional data obtained in the ETT have provided for more exact definition of the correlation.

ETT and DWTT correlations were conducted on a plate of the original Ti-8Al-2Cb-1Ta alloy, and on two heats of Ti-7Al-2Cb-1Ta. The results show the 821 alloy as having good fracture toughness at a YS of 112.2 ksi and the 721 alloys as having poor fracture toughness at slightly lower yield strengths with considerable anisotropy displayed by both materials.

A study is in progress with the aim of optimizing the strength and toughness properties in the Ti-Al-Mo alloy system in the range of 6-7% Al and 2-4% Mo. The results obtained to date indicate a wide variation in fracture toughness with Mo content. Heat-treatment studies of the Ti-6Al-2Mo and other near-alpha alloys are in progress for the same purpose. An exploratory ETT of a Ti-6Al-2Mo alloy that had been given a heat treatment, which the study showed to have a promising combination of high strength and toughness, resulted in an estimated 6-7% strain deformation in the presence of a 2-in. flaw without fracturing.

EXPLOSION TEAR TEST AND DROP-WEIGHT TEAR TEST RESULTS OF 1-INCH-THICK TITANIUM AND TITANIUM ALLOY PLATES

The ETT, developed as a simulated structural prototype element test for high strength quenched and tempered (Q&T) steel plates, is equally effective in evaluating titanium alloy plates. Parameters of the test involve the application of an elastic and/or plastic strain to a test plate with a centerline 2T, through crack. High toughness is indicated by the arrest of the fracture originating from the sharp crack within the test section while the applied load causes a high level of permanent strain deformation in the plate.

Empirical calibrations as a function of the YS of the test plates are necessary to establish the explosive loading conditions that result in a specified strain deformation. Plates 1 in. x 22 in. x 25 in. without flaws are scribed with a diamond point tool, using a surface plate and an adjustable micrometer type height gage to produce a 1/2-in. grid system. After test firing, the plate grid marks are measured with a traveling microscope and the permanent strain deformation in a 2-in. gage section is determined across the plate profile. From the no-flaw ETT data presently available for titanium alloys, it is known that a 29-30-in. explosive stand-off distance will give a 3-5% permanent strain deformation in 110-120 ksi YS material*. Using comparable loading conditions, test plates with 2-in. flaws are test fired at 30°F and the crack propagation distance is determined.

A summary of the ETT data for tests involving 3-5% strain deformations are shown in Table 1 along with the related DWTT data. It should be noted that all the plates were tested in the WR (2) direction except for one T-36 plate, which is so indicated. In Table 1 a comparison of ETT results of some of these materials with and without flaws shows that the flaw has a very detrimental effect on the performance of these materials within the toughness range investigated. Alloys with DWTT energy values less than 2000 ft-lb withstood a 3-5% strain deformation in the ETT under a "no-flaw" condition. The same alloys fractured completely at the same strain deformation level in the presence of a 2-in. flaw.

An ETT and subsequent DWT tests were conducted on a 1 in. x 20 in. x 20-1/2 in. plate of the "original" test material, Ti-8Al-2Cb-1Ta alloy (T-44), designated MQ-4 by the David Taylor Model Basin. It was necessary to heli-arc weld a 2-1/2-in. extension on each end to provide the customary hold-down area. A 2-in. flaw was placed in the plate by the previously described electron beam welding process (1).

---

* The strain deformations measured for specimens containing flaws frequently show higher local strain deformation values than this - whether failure occurs or not; this is due to local necking of the material in the region adjacent to the fracture.

The explosive loading conditions were set for 3-5% strain deformation in the prime plate. The fracture was propagated in both directions 5 to 6 in. beyond the flaw, for an overall 13-in. length. The DWTT at 30°F resulted in energy values of 2250 and 2200 ft-lb for the respective RW and WR directions. The longitudinal and transverse YS was determined to be 104.7 ksi and 112.2 ksi and the ultimate tensile strength (UTS) to be 114.2 and 120.9 ksi respectively. The specimens were Type D (0.313-in. diam.) and a strain rate of 0.002 in./in./min. was used. These results are at variance with earlier published data which indicated somewhat higher values (3).

A 1 in. x 5 in. x 17 in. piece of 7Al-2Cb-1Ta titanium alloy plate (T-33) from Heat No. 30436 was obtained from the U. S. Naval Applied Science Laboratory and was tested on the drop-weight machine where a bracketing technique of complete and incomplete fracturing is required to assess the notch fracture toughness level. Test data showed that the DWTT energy value was slightly below 2000 ft-lb. Another plate, 1 in. x 15 in. x 19 in., of the same heat was obtained and RW and WR DWTT specimens were prepared. The principal rolling direction of the plate was indicated to be in the 15-in. dimension. Duplicate results obtained from each orientation gave DWTT energy values of 1994 and 1961 ft-lb as compared with 1384 and 1384 ft-lb - the higher energy values were obtained for fractures running parallel to the indicated rolling direction. These results show that the principal rolling direction was incorrectly indicated and was actually in the 19-in. dimension. The difference in the DWTT values in the two directions is indicative of anisotropy due to rolling. Plates of a 7Al-2Cb-1Ta titanium alloy (T-39) from Heat No. 30464 also were provided for DWTT and ETT evaluation. The DWTT energy values were found to be 2086 and 1296 ft-lb respectively in the RW and WR orientations. These DWTT results indicate that the fracture toughness properties of the T-33 and T-39 plates are quite similar.

The ETT result of T-39 is shown in Figs. 1a and 1b. The plate was explosion loaded to a 3-5% plastic strain level in the presence of a 3-in. through flaw. As can be seen, the plate completely fractured at the level of loading.

The longitudinal and transverse YS and UTS for T-33 was determined to be 106.6 and 111.7 ksi and 126 and 130 ksi respectively. For T-39 the longitudinal YS and UTS were found to be 106 and 120 ksi respectively.

Test plates of other titanium alloys, such as the 6Al-2Mo, 6Al-4Sn-1V and 8Al-2Cb-1Ta alloys, having DWTT values and yield strengths higher than the Ti-7Al-2Cb-1Ta alloy reported here have been subjected to the same ETT. The higher fracture toughness was confirmed by the ETT by stopping of the fracture within a few inches from the flaw.

CORRELATION OF TENSILE AND FRACTURE TOUGHNESS PROPERTIES FOR 1-INCH-THICK TITANIUM AND TITANIUM ALLOYS

The first preliminary correlation between C_v, DWTT, ETT, and YS was presented in a previous report (1). Subsequent calibrations of titanium alloy plates without flaws indicated that the amount of strain deformation developed in the test increased at a slightly faster rate with increasing explosion load intensity than originally estimated. Therefore, a correction of the earlier correlation has been made and is presented in Fig. 2. It should be noted that a wide range of fracture toughness may be developed by different alloys of the same strength level; however, the maximum for the strength level decreases with increasing strength level. The limiting, ceiling curve has been designated as the "optimum material trend line" (OMTL). This limiting curve may be recognized as the "yardstick" for evaluation of alloys, and as a point of reference for design and for specifications. Explosion tear tests conducted for a limited number of "points" shown in the figure established the pre-fracture strain cut-offs illustrated by the large arrows. By extrapolation to the OMTL, it is deduced that (for presently definable alloys) 135 to 145 ksi is the maximum strength level for which it is estimated to be possible to develop pre-fracture strains in the order of 1-2%.

There is evidence that pre-fracture strain deformations above 5% can be attained for some of the low interstitial titanium alloys if the proper combination of alloying elements and/or heat treatments are established. Incomplete ETT results on an annealed and aged Ti-6Al-2Mo plate (T-22) indicate a 6-7% strain deformation was obtained in the presence of a 2-in. flaw without complete fracturing. The DWTT energy value of the material was 2566 ft-lb.

HEAT-TREATMENT STUDIES ON SOME TITANIUM ALLOYS

Heat-treatment studies on a number of titanium alloys have been continued in order to develop information on the stability of the alloys and to determine the heat treatments which will produce an optimum combination of strength and toughness. The alloys under study include a commercially-produced Ti-6Al-2Mo (T-22) with .07% O_2, NRL-produced Ti-7Al-2Mo (T-29) with ~ .04% O_2, a commercially-produced Ti-8Al-1Mo-1V (T-19), an NRL-produced and INFAB forged-and-rolled Ti-8Al-1Mo-1V (T-28) with

.04% O_2, a commercially-produced Ti-6.5Al-5Zr-1V (T-36), and a Ti-6Al-2Sn-1Mo-1V (T-37) with .08% O_2.

Beta transus temperatures were reported to be 1840°F ± 15°F and 1860°F ± 15°F for the Ti-6Al-2Mo and Ti-7Al-2Mo alloys respectively. The beta transus temperature for the two Ti-8Al-1Mo-1V alloys was found to be 1885°F ± 15°F (Figs.3 and 4). The beta transus temperatures for Ti-6.5Al-5Zr-1V and Ti-6Al-2Sn-1Mo-1V are reported (4) to be approximately 1835°F and 1820°F respectively. These values are presently being checked at NRL.

Charpy V-notch specimens of the Ti-6Al-2Mo, Ti-6.5Al-5Zr-1V, and Ti-6Al-2Sn-1Mo-1V alloys in RW and WR orientations were solution-annealed in argon for one hour at 1750°F to 1800°F, and at 1750°F to 1850°F for the Ti-8Al-1Mo-1V and Ti-7Al-2Mo alloys. The specimens were then air-cooled and aged in argon from 1-4 hours at 1100°F to 1200°F and then, in most cases, water-quenched. All specimens were then tested at -80°F and +32°F. Type D tensile specimens (0.313-in.-diam) of each of these alloys were given the same heat treatments that had produced the better C_v data for each alloy. Tensile tests were conducted at a strain rate of 0.002 in./in./min. A tabulation of the results of Charpy V-notch and tensile tests is presented in Tables 2-7.

Figures 5 and 6 show the effects of solution annealing temperatures (with a common 1100°F age for two hours followed by water quenching) on the Charpy V-notch energy and 0.2% offset YS of the alloy Ti-8Al-1Mo-1V (T-28). Figures 7 and 8 show the effects of solution annealing temperatures (with a common 1200°F age for two hours and water quenching) on the Charpy V-notch energy and YS of the same alloy. It is interesting to note in Figures 6 and 8 that the YS decreases with increasing solution annealing temperatures for the same aging treatment. The 1200°F aging treatment shows a curve nearly parallel to the 1100°F age and approximately 6 ksi higher in yield strengths. Heat treatments for T-28 (Ti-8Al-1Mo-1V) that would warrant further study involve solution annealing temperatures less than 1750°F (1600-1700°F) and subsequent aging at temperatures in excess of 1200°F (1250°F-1300°F).

The fracture toughness values as measured by the Charpy V-notch test for the two Ti-8Al-1Mo-1V alloys with comparable heat treatments are noticeably different. In the as-received condition an analysis of interstitial content showed T-19 to have .07% O_2 in comparison to .05% for the T-28 material. In T-19 the coarseness of the structure, as shown in Fig. 3, for heat treating temperatures below the beta transus would suggest that the material had been rolled at temperatures above the beta transus (1885°F ± 15°F). The T-28 alloy was rolled at 1800°F and exhibits a fine-grained structure, Fig. 4. It appears that the rolling temperature and the interstitial oxygen content may play an important part in determining fracture toughness in this alloy composition. The thermal stability of T-22 and T-29 alloys appears quite good.

Filler wires have been fabricated from a section of the respective material and will be used in studying the welding properties of the two alloys.

WELDING TITANIUM ALLOY PLATE

Preliminary heli-arc welds in Ti-6Al-4Sn-1V, Ti-6Al-2Mo, and Ti-6Al-2Sn-1Mo-1V one-inch plate were prepared in the dry-box for DWT testing. The Ti-6Al-5Zr-1V alloy was also welded; however, the welding wire was mislabeled by the producer and chemical analysis showed it to be the Ti-6Al-2Sn-1Mo-1V composition. Joint preparation consisted of double "V" 30° bevels having a 1/8-in. face and allowance for a 0.45-in. root gap. Welding sequences were compared involving a single pass on both sides with a root pass and a finish pass on both sides. The DWTT results for these weldments are shown below.

DROP-WEIGHT TEAR TEST DATA FOR HELI-ARC WELDED PLATE

Alloy	Single Pass Both Sides (ft-lb)	Root Pass & Filler Pass (ft-lb)
Ti-6Al-4Sn-1V	1418	1540
Ti-6Al-2Mo	1418	1478
Ti-6Al-2Sn-1Mo-1V		1784

Additional weldments are being prepared and will be heat-treated prior to DWT testing.

TITANIUM ALLOY DEVELOPMENT

The promising notch fracture properties obtained to date on a low interstitial commercial heat of Ti-6Al-2.5Mo and an experimental heat of Ti-6.5Al-2Mo suggest the examination of the effects of Mo additions to a high purity Ti-6-7Al alloy base. With a view toward optimizing the alloy composition for toughness and strength, a series of four 10-lb heats of Ti-7Al- plus 2.5,3, 3.5 and 4 wt-% Mo were prepared. Electro-refined titanium, 99.95 Al shot, and Ti-40Mo master alloy cuttings were compacted to form electrodes and double vacuum arc-melted into 4-in.-diam ingots. These ingots were hot-forged at 2000°F to 1-1/4-in. x 4-in. slabs and hot-rolled at 1850°F to 1-in. x 4-in. x 15-in. plate. DWT tests on these plates gave tear energies of 3700, 2800, 3200, and 1750 ft-lb respectively for the as-rolled longitudinal test condition. Comparative DWTT values for the commercial Ti-6Al-2.5Mo and the experimental Ti-6.5Al-2Mo alloys are respectively 3100 and 4000-4300 ft-lb. The chemistry, microstructure, tensile strength, and Charpy V properties of these alloys are being determined.

FRACTURE TOUGHNESS EVALUATION OF 1-IN.-THICK ALUMINUM ALLOY PLATES

(R.J. Goode and R.W. Judy)

Fracture toughness information of any kind for aluminum alloys is very meager. For steels, and to a lesser extent for titanium, the C_v energy values have been calibrated as the results of the NRL studies. For aluminum alloys the C_v energy values are very low and essentially constant over a wide range of temperature; therefore, they have been considered by the metals industry as being of little value for indicating levels of fracture toughness. Fractographic studies (5) have shown that the mode of failure in aluminum alloy plates involves dimple rupture, a ductile mode of fracture. Cleavage fractures, which are associated with brittle failure and with ductile-to-brittle transition behavior over a narrow range of temperatures in conventional structural steels, were not found in plates of pure aluminum or in the alloys 7075 T-4, 2024 T-4, and 6061 T-651.

The purpose of this investigation is to devise simple laboratory methods of determining the fracture toughness characteristics of aluminum alloys in thick sections and to evaluate the significance of the values in terms of prediction of service performance and structural reliability.

Small laboratory tests, including the C_v, tensile, and DWT tests, have been conducted on five aluminum alloys representing a range of strength and toughness levels. Partial results of these tests were reported in the First Quarterly

Report (5). The results presently show that the DWTT is a promising method for measuring the fracture toughness of aluminum alloys.

Table 8 gives the tensile properties of all the alloys tested to date. The results show the wide range of tensile strengths and ductility (reduction of area). Figure 9 presents the results of the standard C_V tests. A plate of pure aluminum (1100) is not represented on this chart because the specimens deformed, rather than breaking, due to the high ductility of the material. The C_V energy values obtained in this test are extremely low when compared to those obtained in testing other medium and high strength structural materials, and they show little discrimination between the alloys tested.

The DWTT shows promise for indicating distinct differences in fracture toughness information of aluminum alloys. This test is designed to measure the energy absorption of materials when fractured in the presence of a sharp crack. The aluminum specimen (Figs. 10 and 11) is a 5 in. x 17 in. section of 1-in. plate with a 1-1/2-in. electron beam crack starter weld at the edge center of the long dimension and completely penetrating through the thickness of the plate. The crack starter weld is embrittled by the addition of iron during welding. The specimen is broken in a 5000 ft-lb pendulum-type impact machine (6) and the energy absorbed by the specimen is recorded. This test has been carried out for each alloy at 30°F in the RW and WR orientations and the results are correlated with the C_V test values and the YS for the same material.

In previous work (5), the crack starter weld for aluminum DWTT specimens was a 1-1/2-in.-deep cut-off wheel slit in the same location as the presently used electron beam weld. This configuration provided a rather blunt notch and required a higher percentage of the total fracture energy to form the initial crack. The brittle electron beam weld provides a very sharp crack with a small amount of specimen deflection, thereby requiring a minimum amount of energy to develop a natural, sharp flaw condition. Another consideration in the use of the brittle weld crack is the similarity to the crack-like defects found in welded structures.

Figure 12 shows that the DWTT energy increases rapidly with increasing Charpy V energy. The DWTT values more clearly show the anisotropy of the 2024 T-4, 6061 T-651, and 5456 T-321 alloy plates than do the C_V values or the tensile ductility data. A wide range of DWTT values are associated with a limited range of low C_V values, indicating that the DWTT energy is a much more sensitive indicator of different levels of fracture toughness for aluminum alloys.

LOW-CYCLE FATIGUE AND CRACK GROWTH RATES IN QUENCHED AND TEMPERED STEELS AT VARIOUS STRENGTH LEVELS

(T.W. Crooker, R.E. Morey, & E.A. Lange)

One of the factors to be considered in the selection of high strength materials is the possibility of fatigue cracks initiating at points of high stress and growing to a dangerous size. This is a complex problem involving design, construction practice, and operating history, as well as the choice of material. However, it is essential that the fatigue characteristics of the various competitive materials be compared on a common basis, which is the purpose of this study.

Since the presence of initial cracks in a cyclically loaded structure is often assured because of the unavoidable consequence of deficiencies in manufacturing and inspection techniques, the most significant material characteristic is considered to be the rate of crack growth under cyclic loading. A deflection-controlled plate bend test was chosen to obtain this information. A detailed description of the experimental procedure is presented in the First Quarterly Report (5). Briefly, a bar-shaped specimen which has a test section 0.5 in. thick and 2.5 in. wide is loaded as a cantilever beam in a hydraulic machine at a rate of 5 cycles per minute. The specimen is of the Lehigh design and the fatigue machine was developed by the U. S. Naval Marine Engineering Laboratory. Since the test concerns the growth of fatigue cracks, initiation of the crack is enhanced by placing a 1/4-in.-long mechanical notch at the center of the reduced section. The length of the crack is measured with an optical micrometer and frequent observations are made in order to monitor the growth rate of the crack along the specimen surface. Nominal surface strains across the test section are measured by means of resistance-type strain gages.

The experimental setup permits close control of test variables, such as deflection and total strain range. Laboratory measurements include total crack length and cycles of applied load. Crack growth rates can be obtained directly from the slope of the resulting plots of these laboratory data, thus enabling this series of tests to evaluate the resistance of various materials to fatigue crack growth under controlled conditions and to determine the effects of such factors as strain range and mean strain.

EXPERIMENTAL PROCEDURE AND MATERIALS

Previous experiments (1, 7, 8) have defined the role of total strain range in controlling low-cycle fatigue crack growth rates. The relationship $\Delta L/\Delta N = K\epsilon_T^4$ has been observed to exist for a variety of quenched and tempered (Q&T) steels for total strain range values between 0.5 and 1.5%. The significance of this relationship is threefold. First, it provides a fundamental insight into the mechanics of low-cycle fatigue crack propagation. Second, it serves as a common denominator for comparing the low-cycle fatigue characteristics of materials in terms of two basic quantities, applied total strain range and the resulting crack growth rate. Finally, the importance of this relationship is enhanced by the fact that the values of total strain range over which it has been observed include those values which commonly occur in practical engineering structures under low-cycle fatigue conditions. An example in support of these findings is shown in Fig. 13, which illustrates the results of low-cycle fatigue tests on full-size steel pressure vessels (9). It can be seen that the total strain ranges reported at points of failure in full-size pressure vessel tests coincides with the total strain ranges employed in the NRL low-cycle fatigue program. Also, the total strain range versus life data, plotted in Fig. 13, falls within a band which has a slope inversely proportional to the fourth power of the total strain range. Since there is an inverse relationship between crack growth rate and life, these data offer generalized confirmation of the relationship $\Delta L/\Delta N = K\epsilon_T^4$.

In an effort to gain further insight into the role of strain in low-cycle fatigue crack growth, the two series of tests considered in this report were undertaken. In the first series, it was desired to determine if there existed a threshold value of total strain range below which low-cycle fatigue cracks would cease to propagate and, if such a point exists, whether it can be reached by extrapolation of previous data. The experimental procedure which followed remained unaltered from previous experiments (1, 8). A fully reversed bending cycle was employed and the total strain range, as determined by resistance-type strain gages, was reduced periodically after intervals of a few thousand cycles until further crack growth could not be detected using an optical micrometer.

For the second series of tests, the bending cycle was changed from a fully reversed cycle in order to evaluate the effect of mean strain on low-cycle fatigue crack growth rates. Several specimens were run in a positive deflection bending cycle which resulted in a mean strain equaling 50% of the total strain range. Once the bending cycle had been established, the experimental procedure remained unaltered from previous experiments.

The materials examined in this report consist of four specially rolled steels with "high-chemistry", HY-80 composition, heat-treated to various strength levels. The compositions of the four steels are given in Table 9. In addition to variations in strength level, the test specimens considered in this report also possess significant variations in fracture toughness due to their orientation with respect to rolling direction. The degree of cross-rolling received by the material is given in Table 10 together with the mechanical properties.

THRESHOLD STRAIN EFFECTS

The results of this series of tests strongly suggest the existence of an "endurance limit" value of strain below which low-cycle fatigue crack propagation is negligible. Figure 14 is a log-log plot of crack growth rate versus total strain range for two Q&T steels in which an attempt was made to gradually reduce applied strain range values until the growth of an existing crack became negligible. An increase in the scatter among the data can be seen at the lower strain range values; however, it is felt that this is largely due to the experimental procedure. Observations indicate that the data tend to deviate from a predictable line under two test conditions, during the initial portions of the test when the crack has just begun to propagate away from the mechanical notch and during the latter portions of the test when the crack is propagating through material that has received considerable fatigue damage. A sequence was followed in obtaining the data points in Fig. 14 whereby the lower points were obtained last. Much of the scatter in that region can be attributed to fatigue damage. Further efforts are being made to develop a clearer understanding of the effects of cumulative fatigue damage under low-cycle conditions involving small plastic strains.

The slow loading rate of the low-cycle fatigue machine requires an excessive period of time to establish a truly dormant condition for a fatigue crack, but the accuracy of the crack length measurement can permit the determination of growth rates pertinent to the low-cycle fatigue range, i.e., less than 100,000 cycles of life.

For the 110-ksi-yield-strength (YS) steel, measurable crack growth was observed at an applied total strain range as low as 1600 micro-inches (0.16%) and for the 150-YS steel, crack growth was observed at a strain range of 2500 micro-inches (0.25%), Fig. 14. For practical purposes, any crack growth rate below 1.0 micro-inches/cycle can be considered negligible for heavy sections of notch tough steels. This criteria means that an existing crack could not grow more than 1/10 in. in 100,000 cycles of load application, which is the upper limit of life for the low-cycle fatigue range. However, it is interesting to note that this arbitrary value of threshold strain (0.28%) approximates the strain range value at points of failure in full-size pressure vessels at points corresponding to a life of 80,000 cycles, which is the high end of the low cycle range. Conditions resulting in crack growth rates of 1.0μ-in./cycle appear to correspond to the upper life boundary for low-cycle fatigue. Thus, for strain levels encountered in low-cycle fatigue, it appears that crack growth rates are to be kept under control rather than reduced to an absolute dormant conditions.

MEAN STRAIN EFFECTS

The introduction of a positive mean strain resulted in a marked reduction in low-cycle fatigue performance, as shown by the data illustrated in Fig. 15. The range of mean strains in these preliminary tests included the full range of elastic strains, and up to 0.5% plastic strain. These data obtained from Q&T steels for two strength levels follow a relationship similar to the fourth power relationship between crack growth rate and total strain range for fully reversed bending conditions which was previously discussed. However, a reduction in low-cycle fatigue life caused by tensile prestrains can be expected on the basis of the increase in the observed crack growth rate. The introduction of a prestrain equaling about 50% of the total strain range resulted in a nearly threefold increase in crack growth rates in Q&T steels for values of total strain ranging from 0.5% to 1.0%.

The importance of this information lies in the fact that mean strain has been shown to be equivalent to prestrain in its effect on low-cycle fatigue performance (10).

Testing of full-size structures, such as pressure vessels (9), has revealed a performance gap between laboratory data and actual service performance. One of the factors which can contribute to this performance gap is mean strain, since the membrane stress cycle in a pressure vessel is zero to tension and the conventional laboratory fatigue test uses a full-reversed cycle. Work is currently underway to extend this background of knowledge to other materials such as aluminum, titanium, and cast alloys, and to a wider range of prestrain.

In summary, the data presented in this report offers further evidence that low-cycle fatigue crack growth is a strain-controlled process which functions in the same manner for a variety of basically similar materials possessing widely differing mechanical properties. The reduction of applied strain can reduce crack growth rates to insignificant proportions. Limiting the maximum range of strain at any point in a structure appears to be the most important control for the prevention of excessive growth of fatigue cracks. These strain range effects appear to be independent of other geometric factors, such as crack size, but do depend upon physical factors, such as fatigue damage and atmosphere.

INVESTIGATION OF FRACTURE TOUGHNESS OF HIGH STRENGTH STEELS CONSIDERED FOR DEEP SUBMERGENCE SUBMARINE HULLS

(P. P. Puzak and K. B. Lloyd)

SPECIALLY PROCESSED HIGH CARBON Q&T STEELS

Although weldability and fabricability considerations as presently envisaged might preclude the use of Q&T steels containing in excess of 0.30% carbon for large submarine hulls that cannot be fully Q&T heat treated after fabrication, such steels are of research interest for yield strength levels in excess of 180 ksi. The potentials for weight savings in non-welded applications such as high pressure air flasks or the use of novel welding techniques make it necessary to consider Q&T steels of high carbon content in the submarine hull steel program. The high carbon content steels are also considered to be potential candidate materials for other service applications such as advanced hydrofoil ships and other applications where heat treatment after fabrication might be feasible.

One of the high carbon Q&T steels for which fracture toughness data were presented in previous investigations (1) was a proprietary nickel-cobalt alloy steel (designated Code A) produced by consumable electrode vacuum melting (CEVM) practices. Although 0.36% C was the composition of the particular steel previously investigated, the proprietary Ni-Co steels containing approximately 0.45% C were designed to develop approximately 250 ksi yield strength when tempered at 400° to 600°F. Yield strength values of approximately 200 ksi for tempering temperatures of 400° to 600°F were previously reported for the 0.36% C-Ni-Co steel because the exploratory investigations did not follow the producers' recommendations for optimum heat treatments for the attainment of high strengths requiring the use of refrigeration (to -120°F) after quenching from the austenitizing temperature. The effects of Q&T heat treatments, with and without refrigeration, on the strength and toughness properties of 0.45% C-Ni-Co steel are presently under investigation with recently procured 1-in. plate material.

The proprietary nickel-cobalt Q&T steels represent a comparatively recent development. Composition modifications involving different carbon contents, and higher Cr-Mo-V contents, to develop secondary hardening characteristics upon tempering in the range of 1000°F, have been under intensive research investigation by the steel producer. One small, 1-in.-thick, plate section received for this study (designated Code G-65) represents one of the lower carbon content grades of the specially processed, proprietary, nickel-cobalt alloy steels. The composition was designed to develop approximately 180 to 190 ksi yield strength upon tempering at 1000°F. Small plate sections of two other high carbon content, specially processed, proprietary alloy steels were also obtained. The chemical compositions of these steels are given in Table 11 which also includes the composition of the previously tested 0.36% C-Ni-Co steel (redesignated herein as No. G-33). The basic compositions of the other high carbon content, proprietary steels are noted to be approximately 1%Si-5%Cr-1%Mo-1/2%V (No. G-52) and 1/2%Ni-1%Cr-1%Mo-0.1%V (No. G-53).

The specially processed, Q&T steel plates had been received in the annealed heat treatment condition. Each plate was cut and prepared into a series of DWTT specimens which were then Q&T heat treated to develop a spectrum of strength levels by tempering individual specimens at different temperatures. In addition to conventional Q&T

heat treatments, isothermal transformation heat treatments at 500°F were conducted to develop a bainitic microstructure in the 0.23% C-Ni-Co steel (No. G-65). Such heat treatments are claimed (by the producer) to develop superior strength and fracture toughness properties in the higher carbon content (0.45%) Ni-Co steels. After DWTT were conducted, the fractured specimens were sectioned to provide the necessary blanks for machining of tensile and Charpy V specimens. The test data for each steel are given in Tables 12-14.

A graphical summary of the changes in strength and toughness values developed by these Q&T steels as a function of the tempering temperatures employed is given in Fig. 16. The data previously reported for the 0.36% C-Ni-Co (No. G-33) steel are repeated in Fig. 16 to provide a comparison of data with that developed by the 0.23% C-Ni-Co (No. G-65) steel. The arrows and legend on the cross-hatched lines, Fig. 16 bottom right, depict the correlations for steels of DWTT energies with ETT performance of the steel in the presence of a 2-in. through-thickness flaw. For comparable tempering temperatures, significantly higher strengths are developed by the high carbon-Cr-Mo-V (No. G-52) steel. However, the very low DWTT energies and C_V values indicate that "flat-break" performance in the 2-in.-flaw ETT would be expected for the high carbon-Cr-Mo-V (No. G-52) steel in all of the heat treatment conditions studied.

With increasing tempering temperatures from 400° to 1000°F, both the 0.23% C-Ni-Co (No. G-65) steel and the Ni-Cr-Mo-V (No. G-53) steel display a continual decrease in ultimate tensile strength with essentially no significant variations in yield strength values. These steels differ, however, with respect to the fracture toughness characteristics developed by tempering from 400° to 1000°F. For all Q&T heat treatments studied, the high carbon-Ni-Cr-Mo-V (No. G-53) steel is characterized by very low DWTT energies. Tempering temperatures of 1100°F or higher are required for this steel to develop DWTT energies over 1000 ft-lb (indicative of a low-level, prefracture plastic strain required for fracture in the 2-in.-flaw ETT). The 0.23% C-Ni-Co (No. G-65) steel develops increasing DWTT energies with increasing tempering temperatures from 400° to 1200°F. As was the case for the 0.36% C-Ni-Co steel, tempering temperatures of 700°F and higher for the 0.23% C-Ni-Co steel result in raising the DWTT energies above 1500 ft-lb (indicative of short fractures at 5 to 7% plastic strain in the 2-in.-

flaw ETT). Optimum strength and toughness properties are noted to be developed by the 0.23% C-Ni-Co steel with the 1000°F tempering treatment as recommended by the producer.

DWTT energies of the bainitic microstructure in the 0.23% C-Ni-Co steel heat treated isothermally at 500°F are approximately double that developed in this steel by the conventional Q&T 500°F treatment. The isothermal heat treatment also resulted in lowering the strength level attainable with this steel from approximately 185 ksi yield to 150 ksi yield. A Q&T treatment at approximately 1125°F would be expected to develop a 150-ksi yield strength level in the 0.23% C-Ni-Co steel with a tempered martensitic microstructure. On the basis of an equivalent 150-ksi yield strength, the tempered martensitic microstructure would develop considerably higher DWTT energies than the bainitic microstructural condition in the 0.23% C-Ni-Co steel. There appears to be no advantage in considering bainitic heat treatments of the 0.23% C-Ni-Co steels in that both the strength and toughness levels are considerably lower than that attainable in this steel with optimum Q&T heat treatments at 1000°F.

A comparison of the drop-weight tear and yield strength relationships of the high carbon steels shown in Tables 12 to 14 with that of the previously tested steels is provided by the graphical summary of data given in Fig. 17.

EXPLOSION TEAR AND DROP-WEIGHT TEAR TESTS OF MARAGING STEELS

Among the new materials of interest to the submarine hull program are the maraging steels. They comprise a considerable variety of new steel compositions which are capable of developing high strength levels by annealing and aging heat treatments. These steels have little similarity to the conventional quenched and tempered (Q&T) steels that rely exclusively upon carbon content to develop specific strength levels. The specific maraging compositions are virtually carbon-free and upon annealing (i.e., cooling or quenching) from austenitizing temperatures (ranging from 1500° to 1900°F) a comparatively soft and ductile martensitic microstructure is developed. The soft martensite is strengthened (hardened) by aging heat treatments at temperatures up to 1000°F. The aging treatment results in the precipitation throughout the martensitic matrix of microscopic particles of complex, intermetallic compounds of the primary alloys with Ti, Al, or Cb. The strength levels developed by the aging heat treatment depend upon the specific steel composition, aging time, and aging temperature.

The maraging steels represent a comparatively recent (within five years) materials development. Most of the available information concerning the properties of these steels was developed with material from relatively small (30 to 100 lb) laboratory melts. The test methods and early applications for maraging steels involved predominantly sheet metal thicknesses. In thin, sheet metal thicknesses, the maraging steels have generally displayed superior toughness properties at ultrahigh strength levels to those developed in conventional Q&T steel alloys of equivalent strengths.

Within the past two to three years, large tonnage (in excess of 10 tons) production heats of maraging steels have been produced for "hardware" applications involving plate thicknesses. These invariably have been limited to the 18% Ni-Co-Mo compositions capable of developing yield strengths in the range of 220 to 300 ksi when aged at 900°F (11). One recent hydrotest failure (12) of a large diameter pressure vessel fabricated with 18% Ni maraging steel plate of 250 ksi yield strength provides ample evidence supporting the contention that sheet metal tests cannot be used to develop criteria suitable for predicting the performance of heavy section plate structures. The apparent low fracture toughness levels of the ultrahigh strength grades of thick maraging steels has resulted in more recent research efforts to develop new maraging steel compositions of lower strengths but higher toughness characteristics. These efforts have generally involved composition modifications of the 18% Ni-Co-Mo grades or the development of a new family of maraging steel compositions containing 10% to 12% Ni with Cr instead of Co as the primary alloys.

To date, fracture toughness evaluations have been completed for twenty maraging steels rolled to 1-in. plates. These were obtained from seven production tonnage heats and thirteen experimental heats of new compositions produced in 1-ton and 1/2-ton sizes for special rolling to 1-in. plate. The chemical compositions, melting practices, and heat sizes of the steels obtained for these studies are given in Table 15. All steels were received in the mill-annealed condition and the aging heat treatments were conducted by the Laboratory after welding fabrication of the drop-weight tear and explosion tear test specimens. The latter tests were conducted with fracture propagation only in the "weak" direction of the rolled plate, but tension, Charpy V, and drop-weight tear tests were conducted in both the "weak" and "strong" orientations. Test data obtained for the steels aged for 3 hours at 900°F, the treatment usually recommended to develop maximum yield strength, are given in Table 16. Annealing temperatures of 1700° and 1900°F were used for some steels because exploratory studies had indicated that slightly better C_v energy absorption values were developed by these steels than when annealed at the customary 1500°F.

In addition to the conventional 3 hours at 900°F aged condition, five of the 18% Ni-Co-Mo steels and one of the 12% Ni-Cr-Mo steels were studied after aging for varying times as given by the data in Table 17. A graphical summary of these data is provided in Fig. 18. The 18% Ni-Co-Mo grades all displayed a significant increase (approximately 20 ksi) in yield strength after 3 hours aging over that developed by the material in a 1-hour aging treatment. Longer times (7 hours) at 900°F resulted in again slightly higher yield strengths from those developed by the 18% Ni-Co-Mo steels aged for 3 hours at 900°F. With increasing strength levels, all of the 18% Ni-Co-Mo steels were characterized by the decreasing toughness levels shown in Fig. 18 by the decreasing DWTT and C_v energies with longer aging times. The 12% Ni-Cr-Mo steel (No. G-35), however, developed only a small (2 to 5 ksi) increase in yield strength upon aging for 3 or 7 hours at 900°F from that developed after aging for 1 hour at 900°F. With the small changes in strength levels, concomitantly small changes in toughess levels were noted to be developed with longer aging times for this 12% Ni-Cr-Mo steel. Investigation of and longer aging times of more steels of this grade are needed to establish whether this behavior is characteristic of all 12% Ni-Cr-Mo maraging steels.

The DWTT energy and yield strength relationships for all the maraging steels tested to date, listed in Tables 16 and 17, are depicted graphically in the summary of data given in Fig. 19. A comparison with previously tested steels is also provided in Fig. 19, by indicating the positions of the optimum materials trend line (OMTL) curves established from previous investigations (1). The data illustrated in Fig. 19 for the maraging steels of approximately 190 ksi yield strength and in Fig. 17 for specially processed Q&T steels of approximately 170 ksi yield strength depict higher practicable upper limits of fracture toughness than that obtained in previous investigations with steels of similar strengths. For any given strength level, the practicable limit of fracture toughness depicted by the OMTL was shown to be a function, not only of chemical composition and heat treatment employed, but also of mill processing variables (cross-rolling and melting practices).

A general summary of all steel data developed to date is given in Fig. 20 with the OMTL for specially processed steels adjusted to correspond with the data presented herein. The DWTT data given in this illustration represent values established with fracture propagation in the "weak" direction of the various steel plates. All steels of 210 ksi and higher yield strength levels tested to date have been characterized by comparatively low DWTT energies ranging from approximately 400 to 800 ft-lb. Investigations of more steels with yield strengths ranging from 200 to 260 ksi are needed to provide a better definition of the OMTL for this strength level range. By extrapolation to the OMTL curves given in Fig. 20 for presently defined steels, the maximum yield strength levels for which the development of 2 to 5% pre-fracture strains would be possible in the 2-in.-flaw ETT is estimated to be approximately 175 ksi yield strength for conventionally processed steels and 225 ksi yield strength for specially processed steels.

REFERENCES

1. Puzak, Lloyd, Goode, Huber, Howe, Crooker, and Lange, "Metallurgical Characteristics of High Strength Structural Materials (Third Quarterly Report)," NRL Report 6086, Jan. 1964

2. ASTM Materials and Research Standards, Vol. 1, No. 5, May 1961

3. Willner, A.R., and Sullivan, V.E., "Metallurgical Investigation of Titanium Alloys for Application to Deep-Diving Submarines," DTMB Progress Report 1482, Dec. 1960

4. Day, D.L., "Development of Titanium Alloys for Submarine Plate Applications," TMCA Report TTL-61, Nov. 8, 1963

5. Puzak, Lloyd, Lange, Goode, Huber, Dahlberg, and Beachem, "Metallurgical Characteristics of High Strength Structural Materials (First Quarterly Report)," NRL Memorandum Report 1438, June 1963

6. Goode, R.J., Huber, R.W., and Kuntz, A.J., pp. 16-18 in "Report of NRL Progress," Mar. 1964

7. Puzak, Lloyd, Lange, Goode, and Huber, "Metallurgical Characteristics of High Strength Structural Materials (Second Quarterly Report)," NRL Memorandum Report 1461, Sept. 1963

8. Crooker, T.W., Morey, R.E., and Lange, E.A., "Plastic Flow Processes (Low-Cycle Fatigue Crack Propagation)," pp. 37-38 in "Report of NRL Progress," Dec. 1963

9. Kooistra, L.F., Lange, E.A., and Pickett, A.G., "Full-Size Pressure Vessel Testing and Its Application to Design," ASME Paper No. 63-WA-293

10. Gerberich, W.W., "An Analysis of Several of the Variables Encountered in Low-Cycle Fatigue," Syracuse University Research Institute Report MET 575-5961T4, June 1959

11. Drennan, D.C., and Roach, C.B., "Properties of Maraging Steels," DMIC Memorandum 156, July 1962

12. Bhat, G.K., "Metallurgical Analysis of Fractured Closure Plate of the 120-Inch Maraging Steel Prototype Vessel," LPC Report 609-P-8, Research Contract Status Report 8 under Air Force Contract AF 04(611)-8525, Nov. 1963

TABLE 1

SUMMARY OF DROP-WEIGHT TEAR TEST AND EXPLOSION TEAR TEST RESULTS ON SOME TITANIUM ALLOY PLATES

Alloy No.	Nominal Composition	Plate Condition	Rolling Direction	DWTT Drop-Weight Machine (ft-lb)	DWTT Impact Machine (ft-lb)	Flaw	ETT Results (3-5% Strain Deformation)
T-20	6Al-4Sn-1V	As Received- Mill Annealed	RW WR	2000-2500 <1500			
		1800°F/2hr	RW		3050	2"	5-1/2" Fract.
		1800°F/2hr(ETT Plate)	RW WR		2000-2260 1230-1420	2"	CompleteFract.
T-21	6Al-6V-2.5Sn	As Received- Mill Annealed	RW & WR	<1000		2"	Flat Fracture -Several pcs.
		1660°F/2hr(ETT Plate)	WR	1500-2000		2"	Compl. Fract.
T-22	6Al-2Mo	As Received- Hot Rolled 1700°F- Annealed 1350°F/8hr	RW & WR	1500-2000			Compl. Fract.
		1800°F/2hr	RW		3100		
		1800°F/2hr(ETT Plate)	RW WR	2500	2100-2440	2"	3" Fracture
T-23	8Al-2Cb-1Ta	As Received	RW & WR WR WR	1500-2000	1650-1750	None 1" 2"	No Fracture Compl. Fract. Compl. Fract.
T-28B	8Al-1Mo-1V	INFAB-As Rolled	RW		1850		
		1820°F-1880°F/2hr	RW		3940-4400		
		1850°F/1hr	WR			2"	8" Fracture
T-29	7Al-2Mo	INFAB-As Rolled			4130		
		1820-1850°F/2hr			4000-4300		
		1800°F/1hr				2"	8" Fracture
T-36	6.5Al-5Zr-1V	As Received- Mill Annealed	RW WR		1480	None None	No Fracture No Fracture
		As Received- Mill Annealed	WR		1480	2"	Compl. Fract.
		1750°F/2hr	WR		1410	2"	Compl. Fract.
T-37	6Al-2Sn-1Mo	As Received	WR WR		1440	None 2"	No Fracture Compl. Fract.
		1750°F/2hr	RW WR		2150	2"	Compl. Fract.
T-39	7Al-2Cb-1Ta	As Received	RW WR		2090 1300	2"	Compl. Fract.
T-44	8Al-2Cb-1Ta	As Received (DTMB MQ-4)	RW WR		2260 2210	2"	10" Fracture

TABLE 2

TEST DATA FOR SOLUTION ANNEALING AND AGING TREATMENTS ON THE ALLOY Ti-6Al-2Mo (T-22) (Beta transus 1840°F±15°F)

Solution Heat Treatment	Aging Heat Treatment	Longitud. (RW) C_V Impact Energy (ft-lbs) -80°F	Longitud. (RW) C_V Impact Energy (ft-lbs) +32°F	Transverse (WR) C_V Impact Energy (ft-lbs) -80°F	Transverse (WR) C_V Impact Energy (ft-lbs) +32°F	YS (0.2%) (ksi)	UTS (ksi)	Elong (%)	RA (%)
As Received		16.0	20.0	16.0	19.5				
1800°F/1hr/AC	--	37.5	54.0	34.0	57.0	115.8(L)	125.7(L)	12.9	40.3
1800°F/1hr/AC	1100°F/1hr/WQ	23.0	38.0	24.5	49.0	115.7(L)	125.5(L)	12.9	35.8
1800°F/1hr/AC	1200°F/1hr/WQ	29.0	55.5	34.0	45.5	120.6(T)	126.1(T)	12.9	36.4
1800°F/1hr/AC	1200°F/2hr/WQ	29.5	39.5	28.0	40.5	124.8(T)	130.1(T)	11.8	32.3
1750°F/1hr/AC	1100°F/1hr/WQ	21.0	34.0	22.0	31.5	126.1(T)	135.9(T)	13.6	27.8
1750°F/1hr/AC	1100°F/2hr/WQ	36.0	40.0	31.5	35.5	126.3(L)	131.9(L)	12.1	34.7
1750°F/1hr/AC	1200°F/4hr/WQ	26.0	37.0	26.5	34.0	123.5(L)	126.1(L)	13.6	40.2

TABLE 3

TEST DATA FOR SOLUTION ANNEALING AND AGING TREATMENTS ON THE ALLOY Ti-8Al-1Mo-1V (T-28)*

Solution Heat Treatment	Aging Heat Treatment	Longitdnl (RW) C_v Impact Energy (ft-lbs)		Transverse (WR) C_v Impact Energy (ft-lbs)		YS (0.2%) (ksi)	UTS (ksi)	Elong (%)	RA (%)
		-80°F	+32°F	-80°F	+32°F				
As Received		37.0	46.0	30.0	36.5				
1850°F/1hr/AC	1100°F/2hr/WQ	66.0	67.0	35.5	51.0	104.7(T)	117.7(T)	12.1	25.1
1850°F/1hr/AC	1200°F/2hr/WQ	69.0	66.5	47.0	69.0	107.9(L) 107.3(T)	117.0(L) 116.8(T)	8.6 9.3	16.0 13.6
1850°F/1hr/AC	--					110.2(T)	122.2(T)	12.9	26.7
1800°F/1hr/AC	1100°F/2hr/WQ	58.5	63.0			106.0(T)	116.7(T)	16.4	32.1
1800°F/1hr/AC	1200°F/2hr/WQ	67.0	59.0	40.0	40.5	111.8(T) 113.8(L)	120.9(T) 123.9(L)	13.6 12.9	29.9 21.2
1800°F/1hr/AC	--					112.6(T)	127.6(T)	11.4	20.4
1750°F/1hr/AC	1100°F/2hr/WQ			34.0	40.5	112.9(T)	120.4(T)	10.0	31.1
1750°F/1hr/AC	1200°F2hr/WQ	48.0	56.5			119.3(T)	128.75(T)	10.7	23.9
1750°F/1hr/AC	--					111.25(T)	124.7(T)	10.7	24.6
1750°F/1hr/AC	1200°F/4hr/WQ	26.5	33.0	27.5	39.5	116.8(L)	123.4(L)	6.4	24.0
1820°F/2hr/AC	--	26.5	30.0						

* Beta transus 1885°F ± 15°F

TABLE 4

TEST DATA FOR SOLUTION ANNEALING AND AGING TREATMENTS ON THE ALLOY Ti-7Al-2Mo (T-29)*

Solution Heat Treatment	Aging Heat Treatment	Longitd'l (RW) C_v Impact Energy (ft-lbs)		Transverse (WR) C_v Impact Energy (ft-lbs)		YS (0.2%) (ksi)	UTS (ksi)	Elong (%)	RA (%)
		-80°F	+32°F	-80°F	+32°F				
As Received			43.0						
1850°F/1hr/AC				31.5	51.0				
1825°F/1hr/AC				43.0	64.0				
1825°F/1hr/AC	1100°F/1hr/WQ			47.0	49.5				
1825°F/1hr/AC	1200°F/1hr/WQ			53.5	59.5				
1800°F/1hr/AC		55.0	63.5	55.0	53.0				
1800°F/1hr/AC	1100°F/1hr/WQ	39.5	48.0	61.5	57.5	96.9(L)	114.8(L)	11.4	23.4
1800°F/1hr/AC	1100°F/4hr/WQ	46.0	56.5	47.0	55.0	96.2(L) 112.2(T)	117.9(L) 125.5(T)	10.7 **	24.8 26.0
1800°F/1hr/AC	1200°F/1hr/WQ			49.0	57.0	98.5(L)	115.1(L)	12.9	32.6
1800°F/1hr/AC	1200°F/4hr/WQ			54.5	51.0	104.7(L)	118.5(L)	11.4	39.8
1750°F/1hr/AC	1100°F/1hr/WQ	51.0	56.0	48.0	57.0	105.3(L) 111.9(T)	119.3(L) 125.3(T)	11.4 12.1	31.6 25.0
1750°F/1hr/AC	1100°F/4hr/WQ	50.5	54.0	52.5	54.0	108.9(T)	121.6(T)	11.4	23.4
1750°F/1hr/AC	1200°F/1hr/WQ	46.0	51.0	52.5	57.5	111.8(L)	122.2(L)	11.4	31.1
1750°F/1hr/AC	1200°F/4hr/WQ	52.5	55.0	45.5	60.0	105.3(L) 111.3(T)	118.7(L) 119.8(T)	10.0 12.9	29.9 34.2

* Beta transus 1860°F ± 15°F

** Broke at index mark

TABLE 5

EFFECTS OF SOLUTION ANNEALING AND AGING TREATMENTS
ON THE ALLOY Ti-8Al-1Mo-1V (T-19)*
AS MEASURED BY THE CHARPY V-NOTCH TEST

Solution Heat Treatment	Aging Heat Treatment	Longitudinal (RW) C_V Impact Energy (ft-lb)		TRANSVERSE (WR) C_V Impact Energy (ft-lb)	
		-80°F	+32°F	-80°F	+32°F
As Received		19.0	23.0	19.0	24.5
1850°F/1hr/AC		30.5	40.5	32.0	45.0
1850°F/1hr/AC	1100°F/2hr/WQ	31.0	37.0	30.0	40.0
1850°F/1hr/AC	1200°F/2hr/WQ	31.5	34.0	28.0	37.5
1800°F/1hr/AC		29.0	40.0	32.5	46.0
1800°F/1hr/AC	1100°F/2hr/WQ	27.5	37.0	31.5	36.5
1800°F/1hr/AC	1200°F/2hr/WQ	28.0	36.0	27.5	34.0
1750°F/1hr/AC				32.0	46.5
1750°F/1hr/AC	1100°F/2hr/WQ	30.5	38.0	30.0	36.0
1750°F/1hr/AC	1200°F/2hr/WQ			28.0	41.5

* Beta transus 1885°F ± 15°F

TABLE 6

EFFECTS OF SOLUTION ANNEALING AND AGING TREATMENTS
ON THE ALLOY Ti-6.5Al-5Zn-1V (T-36)
AS MEASURED BY THE CHARPY V-NOTCH TEST

Solution Heat Treatment	Aging Heat Treatment	Transverse (WR) C_V Impact Energy (ft-lb)	
		-80°F	+32°F
As Received		13.0	17.0
1800°F/1hr/AC	1200°F/1hr/WQ	12.5	17.0
1800°F/1hr/AC	1200°F/4hr/WQ	11.5	17.0
1800°F/1hr/AC	1100°F/2hr/WQ	15.0	22.0
1750°F/1hr/AC	1200°F/2hr/WQ	11.5	16.0
1750°F/1hr/AC	1100°F/1hr/WQ	14.5	22.0
1750°F/1hr/AC	1100°F/4hr/WQ	13.5	20.5

TABLE 7

EFFECTS OF SOLUTION ANNEALING AND AGING TREATMENTS ON THE ALLOY Ti-6Al-2Sn-1Mo-1V (T-37) AS MEASURED BY THE CHARPY V-NOTCH TEST

Solution Heat Treatment	Aging Heat Treatment	Transverse(WR) C_V Impact Energy(ft-lbs)	
		-80°F	+32°F
As Received			27.0
1800°F/2hr/AC		26.0	32.0
1800°F/1hr/AC	1200°F/1hr/WQ	31.5	37.0
1800°F/1hr/AC	1200°F/4hr/WQ	28.0	35.0
1800°F/1hr/AC	1100°F/2hr/WQ	34.0	35.5
1750°F/1hr/AC	1200°F/2hr/WQ	28.5	40.0
1750°F/1hr/AC	1100°F/1hr/WQ	31.5	41.0
1750°F/1hr/AC	1100°F/4hr/WQ	27.5	37.5

TABLE 8

TENSILE PROPERTIES OF ALUMINUM ALLOYS

Alloy No.	Direction	Ultimate Tensile Strength (ksi)	Yield Strength (ksi)	Elong in 2" GL (%)	Reduction of Area (%)
1100F*	L	13.0	9.84	34.0	85.2
2024 T-4	L	71.7	48.0	18	23
	T	71.9	47.8	16	20
5456 H-321*	L	54.1	37.8	12	21.8
	T	55	34.0	16	22.0
6061 T-651	L	45.7	41.7	19	52
	T	47.0	40.0	14	32
7075 T-6	L	90.0	78.5	12	20
	T	88.2	77.8	10	13

* Average of two specimens

TABLE 9

CHEMICAL COMPOSITION
of
SPECIALLY ROLLED AND HEAT-TREATED HY-80 STEELS

Code/YS	Composition - Wt. %							
	C	Mn	Si	P	S	Ni	Cr	Mo
E84/88	.19	.20	.23	.007	.007	2.18	1.29	.30
F60/132*	.20	.35	.32	.007	.010	3.20	1.69	.70
F65/157*	.19	.32	.33	.006	.013	3.28	1.69	.70
F66/117*	.20	.32	.33	.006	.012	3.04	1.58	.78

* Q&T Heat-treated to develop minimum YS levels of 130 and 150 ksi

TABLE 10

MECHANICAL PROPERTIES TEST DATA FOR
SPECIALLY ROLLED AND HEAT-TREATED HY-80 STEELS

Code	Cross-Roll	Direction of Test*	0.505"-dia TensionTest				C_v (30°F) (ft-lb)	DWT (30°F) (ft-lb)
			0.2% YS (ksi)	T.S. (ksi)	Elon. in 2" (%)	R.A. (%)		
E-84	Highly Cross-Rolled	Weak Strong	85.8 90.5	102.7 105.7	22.8 24.0	67.6 70.8	93 115	5000 6200
F60	Straight	Weak Strong	131.8 132.0	151.6 151.2	14.5 19.0	45.8 66.8	30 82	1250 5750
F65	6.2 to 1	Weak Strong	158.0 156.6	175.6 175.2	12.5 17.0	41.3 54.6	23 48	1000 3250
F66	Straight	Weak Strong	116.0 117.8	134.4 135.3	20.8 16.5	68.4 50.6	42 86	2000 6250

*Note: Test direction is defined in terms of fracture path in specimen; i.e., "weak" = specimen fracture parallel to principal (or final) rolling direction, "strong" = specimen fracture transverse to principal (or final) rolling direction.

TABLE 11

CHEMICAL COMPOSITIONS OF SPECIAL MELT PRACTICE Q&T STEELS

Steel No.	Composition - Wt.-%									
	C	Mn	Si	P	S	Ni	Cr	Mo	V	Co
G-33	0.36	0.09	0.01	0.004	0.004	8.40	0.46	0.33	N.D.*	3.5
G-65	0.23	0.26	0.01	0.004	0.002	8.60	0.58	0.50	N.D.*	3.6
G-52	0.41	0.31	0.82	0.008	0.008	0.16	4.89	1.28	0.44	--
G-53	0.47	0.54	0.20	0.006	0.002	0.61	1.13	1.16	0.10	--

* N.D. = Not determined

TABLE 12

TEST DATA FOR SPECIALLY PROCESSED PROPRIETARY HIGH CARBON Cr-Mo-V STEEL--CODE G-52

(Austenitized 1 hr. 1850°F; air-cooled; tempered 2+2 hrs. except 1025°F as noted)

Tempering Temperature (°F)	Direction of Test*	0.505" Dia. Tension Test Data				Rc Hardness	Charpy V at 30°F (ft-lb)	Drop-weight tear at 30°F (ft-lb)
		0.2% Y.S. (ksi)	T.S. (ksi)	El. in 2" (%)	R.A. (%)			
600	Weak	232.8	296.6	7.0	16.2	56.8	11.0	--
600	Strong	240.3	298.5	8.0	18.6	56.8	13.0	--
**1025	Weak	244.2	294.6	8.0	25.6	56.0	7.0	397
**1025	Strong	249.0	294.9	6.8	19.8	56.2	8.5	397
1050	Weak	242.9	294.0	7.8	21.7	55.8	6.6	--
1050	Strong	247.0	283.9	7.8	20.5	54.0	8.3	--
1100	Weak	211.0	245.2	7.0	17.1	49.8	8.3	397
1100	Strong	222.0	257.8	6.0	14.8	52.0	6.0	397
1150	Weak	169.8	203.0	9.0	22.0	43.0	11.0	593
1150	Strong	168.1	200.4	9.5	23.8	42.0	10.0	511

*NOTE: Test direction is defined in terms of fracture path in specimen; i.e., "Weak" = specimen fracture parallel to principal (or final) rolling direction; "Strong" = specimen fracture transverse to principal (or final) rolling direction.

**NOTE: Austenitized 1850°F 30 min.--air-cooled--tempered 2+2 hr.

TABLE 13

TEST DATA FOR SPECIALLY PROCESSED PROPRIETARY HIGH CARBON Ni-Cr-Mo-V STEEL--CODE G-53

(Austenitized 1 hr. 1600°F; air-cooled; tempered 2+2 hrs. except 950°F as noted)

Tempering Temperature (°F)	Direction of Test*	0.505-in. Dia. Tension Test Data				Rc Hardness	Charpy V at 30°F (ft-lb)	Drop-Weight tear at 30°F (ft-lb)
		0.2% Y.S. (ksi)	T.S. (ksi)	El. in 2" (%)	R.A. (%)			
400	Weak	176.0	237.5	10.0	35.0	42.5	18	455
400	Strong	179.4	239.6	11.8	38.1	--	19	--
500	Weak	--	235.6	11.0	42.6	47.5	16	514
500	Strong	181.6	235.4	13.0	47.3	--	14	612
600	Weak	182.0	233.7	12.0	46.6	46.5	13	455
600	Strong	177.4	228.0	12.8	46.2	--	15	621
700	Weak	185.2	228.5	12.8	43.8	48.0	20	--
700	Strong	181.1	224.8	12.5	42.6	--	19	--
800	Weak	178.8	217.3	12.8	44.0	45.0	17	573
800	Strong	181.1	218.1	13.4	45.0	--	18	629
900	Weak	--	213.3	13.9	44.0	45.0	22	301
900	Strong	180.7	213.8	14.1	44.7	--	19	416
**950	Weak	225.6	247.9	11.5	36.8	52.0	18	709
1000	Weak	190.7	216.1	16.0	48.8	47.0	19	612
1000	Strong	186.6	214.8	16.5	49.7	--	18	758
1100	Weak	183.6	205.4	15.0	49.2	44.5	24	1418
1200	Weak	129.8	150.1	18.3	56.9	33.5	~60	--

* NOTE: Test direction is defined in terms of fracture path in specimen: i.e.,
"Weak" = specimen fracture parallel to principal (or final) rolling direction;
"Strong" = specimen fracture transverse to principal (or final) rolling direction.

** NOTE: 950°F = Weak direction; austenitized 1 hr. 1600°F; quenched in salt at 410°F 5 min. air-cooled; tempered 950°F 4 hrs. air-cooled.

TABLE 14

TEST DATA FOR SPECIALLY PROCESSED CEVM PROPRIETARY Ni-Co STEEL--CODE G-65

Tempering Temperature (°F)	Direction of Test*	0.505-in. Dia. Tension Test Data				Charpy V at 30°F (ft-lb)	Drop-weight tear at 30°F (ft-lb)
		0.2% Y.S. (ksi)	T.S. (ksi)	El. in 2" (%)	R.A. (%)		
400	Weak	184.7	235.8	14.0	48.7	36	1108
400	Strong	--	--	--	--	38	--
500	Weak	187.7	225.2	12.7	43.9	31	1412
500	Strong	--	--	--	--	33	--
**500	Weak	149.3	194.5	14.7	53.3	45	2381
**500	Strong	--	--	--	--	56	--
***500	Weak	149.7	195.3	14.2	53.7	42	2440
***500	Strong	--	--	--	--	53	--
700	Weak	183.5	206.1	12.8	50.8	29	1596
700	Strong	--	--	--	--	31	--
900	Weak	182.7	199.1	15.0	51.3	36	1991
900	Strong	--	--	--	--	37	--
1000	Weak	185.2	198.7	16.0	53.5	41	3361
1000	Strong	--	--	--	--	44	--
1100	Weak	171.8	187.9	16.3	52.5	46	>5034
1200	Weak	108.8	180.0	19.8	50.5	53	>5034
1200	Strong	--	--	--	--	57	--

* Test direction is defined in terms of fracture path in specimen: i.e., "Weak"=specimen fracture parallel to principal (or final) rolling direction; "Strong"=specimen fracture transverse to principal (or final) rolling direction.

NOTE: All steels austenitized 1550°F--1 hr--oil quenched and tempered 2+2 hr. & air-cooled expect:

** Austenitized 1550°F--1 hr--quenched in 500°F salt bath--hold 5 hrs & air-cooled; and

**** Austenitized 1550°F--1 hr--quenched in 500°F salt bath--hold 5 hrs--oil quenched. Retemper 500°F--2 hrs--air-cooled.

TABLE 15

CHEMICAL COMPOSITIONS OF MARAGING STEELS

Steel	Melt practice & heat size	Composition - Wt. %										
		Ni	Cr	Co	Mo	Ti	Al	C	Mn	P	S	Si
F83	CEVM-1/2 ton	10.0	5.39	--	3.45	.12	.26	.015	.05	.005	.005	.08
F54	CEVM-1 ton	12.0	3.00	--	3.15	.19	.19	.023	.03	.004	.010	.06
F58	Air -1 ton	12.0	2.86	--	3.20	.12	.19	.015	.03	.005	.010	.08
F82	CEVM-1/2 ton	11.8	3.35	--	3.65	.12	.15	.021	.05	.003	.005	.07
F70	Air-1/2 ton	12.3	3.54	--	3.15	.13	.12	.023	.02	.005	.005	.04
F55	CEVM-1 ton	12.0	4.91	--	3.15	.18	.21	.015	.03	.004	.010	.09
G35	Air-20 ton	11.8	5.28	--	3.35	.12	.12	.027	.10	.004	.004	.10
F69	CEVM-1/2 ton	18.0	--	8.4	2.15	.16	.06	.011	.02	.002	.005	.03
G19	Air-80 ton	18.0	--	8.1	2.72	.12	.14	.019	.04	.003	.008	.02
C36	Air-80 ton	17.6	--	8.1	2.85	.08	.15	.017	.02	.004	.002	.02
G66	CEVM-1 ton	17.8	--	8.1	2.35	.20	.15	.020	.00	.005	.003	.01
G67	CEVM-1 ton	18.3	--	8.1	2.35	.20	.16	.020	.00	.005	.003	.01
F56	CEVM-1 ton	18.0	--	8.7	3.38	.18	.09	.015	.03	.004	.018	.01
F59	Air-1 ton	18.2	--	8.7	3.25	.16	.10	.007	.02	.005	.010	.01
G57	CEVM-15 ton	17.0	--	7.7	4.80	.36	.08	.020	.04	.004	.003	.10
D63	Air-10 ton	18.3	--	7.4	5.30	.24	.12	.040	.03	.001	.004	.08
F84	CEVM-1/2 ton	17.4	--	7.7	5.20	.32	.10	.025	.05	.005	.007	.13
G56	CEVM-15 ton	17.8	--	7.7	4.95	.24	.04	.020	.03	.004	.003	.01
F57	CEVM-1 ton	18.0	--	9.1	5.05	.76	.16	.007	.02	.004	.010	.06
G77	CEVM-15 ton	17.4	--	9.1	4.85	.68	.23	.020	.04	.005	.002	.12

TABLE 16

TEST DATA FOR MARAGING STEELS

(All steels aged 3 hrs. at 900°F)

Steel No	Anneal (°F)	Direction of test	0.505" Dia tension test data: 0.2% Y.S. (ksi)	T.S. (ksi)	El. in 2" (%)	R.A. (%)	Charpy V at 30°F (ft-lb)	Drop-weight tear at 30°F (ft-lb)
F-83	1500	Weak	154.4	156.2	18.0	67.3	97	5750
F-83	1500	Strong	157.2	160.7	15.3	63.7	102	7250
F-54	1700	Weak	146.3	154.3	15.5	61.7	64	3750
F-54	1700	Strong	148.1	158.2	16.0	64.1	104	4250
F-58	1900	Weak	152.4	161.9	14.5	61.7	51	3250
F-58	1900	Strong	150.2	162.1	15.8	62.2	70	3500
F-82	1500	Weak	139.7	141.5	18.3	67.2	99	5500
F-82	1500	Strong	146.3	148.5	16.8	66.3	108	6750
F-70	1500	Weak	147.9	151.3	16.3	63.9	71	3750
F-70	1500	Strong	144.9	148.5	17.5	64.0	80	5500
F-55	1900	Weak	162.5	174.8	14.3	60.0	57	3500
F-55	1900	Strong	161.9	175.2	15.0	63.1	84	4750
G-35	1500	Weak	184.8	190.4	13.5	41.0	34	1662
G-35	1500	Strong	--	--	--	--	35	--
F-69	1500	Weak	155.5	163.5	15.3	67.4	99	3750
F-69	1500	Strong	156.0	163.3	15.3	66.8	109	4750
G-36	1500	Weak	179.0	187.6	13.0	53.6	32	870
G-36	1500	Strong	--	--	--	--	34	--
F-56	1500	Weak	204.2	212.2	12.0	59.8	33	1250
F-56	1500	Strong	200.4	209.2	13.0	62.5	45	1750
F-59	1500	Weak	201.3	208.9	12.0	57.6	33	1000
F-59	1500	Strong	200.9	208.6	12.0	56.3	36	1250
G-57	1500	Weak	217.5	224.4	12.0	56.6	34	683
G-66	1500	Weak	192.4	197.5	13.8	61.4	46	3866
G-66	1500	Strong	190.4	197.3	13.5	58.0	53	>5000
G-67	1500	Weak	190.3	197.2	13.3	58.0	45	3820
G-67	1500	Strong	193.2	198.8	13.5	63.0	51	>5000
D-63	1500	Weak	--	--	--	--	20	<500
D-63	1500	Strong	229.5	240.3	9.0	45.9	24	<500
D-63	1750	Weak	234.5	245.7	7.0	29.2	--	<500
F-84	1500	Weak	259.6	266.1	9.5	49.0	21	<500
F-84	1500	Strong	248.5	254.9	10.0	49.0	22	<500
G-56	1500	Weak	263.0	271.8	9.0	40.8	13	453
F-57	1500	Weak	279.8	293.6	8.5	42.5	14	<500
F-57	1500	Strong	285.6	293.9	4.8	19.2	18	<500
G-77	1500	Weak	284.0	297.1	5.5	27.7	16	337

TABLE 17

TEST DATA FOR MARAGING STEELS

Steel No.	Anneal (°F)	Aged (hr.)	Aged (°F)	Direction of test	0.505" dia. tension test data 0.2%Y.S. (ksi)	T.S. (ksi)	El. in 2" (%)	R.A. (%)	Charpy V at 30°F (ft-lb)	Drop-weight tear at 30°F (ft-lb)
G-35	1500	1	900	Weak	183.1	189.7	14.0	57.0	36	1506
G-35	1500	1	900	Strong	--	--	--	--	37	--
G-35	1500	3	900	Weak	184.8	190.4	13	54.5	34	1662
G-35	1500	3	900	Strong	--	--	---	--	35	--
G-35	1500	7	900	Weak	187.9	193.5	13.0	55.2	31	1228
G-35	1500	7	900	Strong	--	--	--	--	33	--
G-19	1700	2	850	Weak	159.5	173.1	14.0	54.2	35	1750
G-19	1700	2	850	Strong	164.5	176.2	14.5	59.6	45	2000
G-19	1700	5	850	Weak	173.6	185.2	13.0	53.7	32	1250
G-19	1700	5	850	Strong	176.2	184.6	15.5	59.4	38	1750
G-19	1700	7	900	Weak	186.4	194.4	11.5	47.8	28	710
G-19	1700	7	900	Strong	189.1	197.5	13.0	56.5	32	1080
G-36	1500	1	900	Weak	167.4	176.6	14.3	56.5	37	987
G-36	1500	1	900	Strong	--	--	--	--	38	--
G-36	1500	3	900	Weak	179.0	187.6	13.0	53.6	32	870
G-36	1500	3	900	Strong	--	--	--	--	35	--
G-36	1500	7	900	Weak	192.7	200.0	12.0	50.5	28	601
G-36	1500	7	900	Strong	--	--	--	--	33	--
G-57	1500	1	900	Weak	185.6	193.8	13.8	60.9	43	1840
G-57	1500	3	900	Weak	217.5	224.4	12.0	55.6	34	683
G-57	1500	7	900	Weak	226.6	233.3	11.8	55.9	29	668
G-56	1500	1	900	Weak	223.0	234.1	10.5	45.1	16	570
G-56	1500	3	900	Weak	263.0	271.8	9.0	40.8	13	453
G-56	1500	7	900	Weak	266.8	277.4	6.0	25.9	14	395
G-77	1500	1	900	Weak	247.2	258.5	8.5	35.0	17	453
G-77	1500	3	900	Weak	284.0	297.1	5.5	27.5	16	337
G-77	1500	7	900	Weak	296.5	303.3	5.7	24.2	15	395

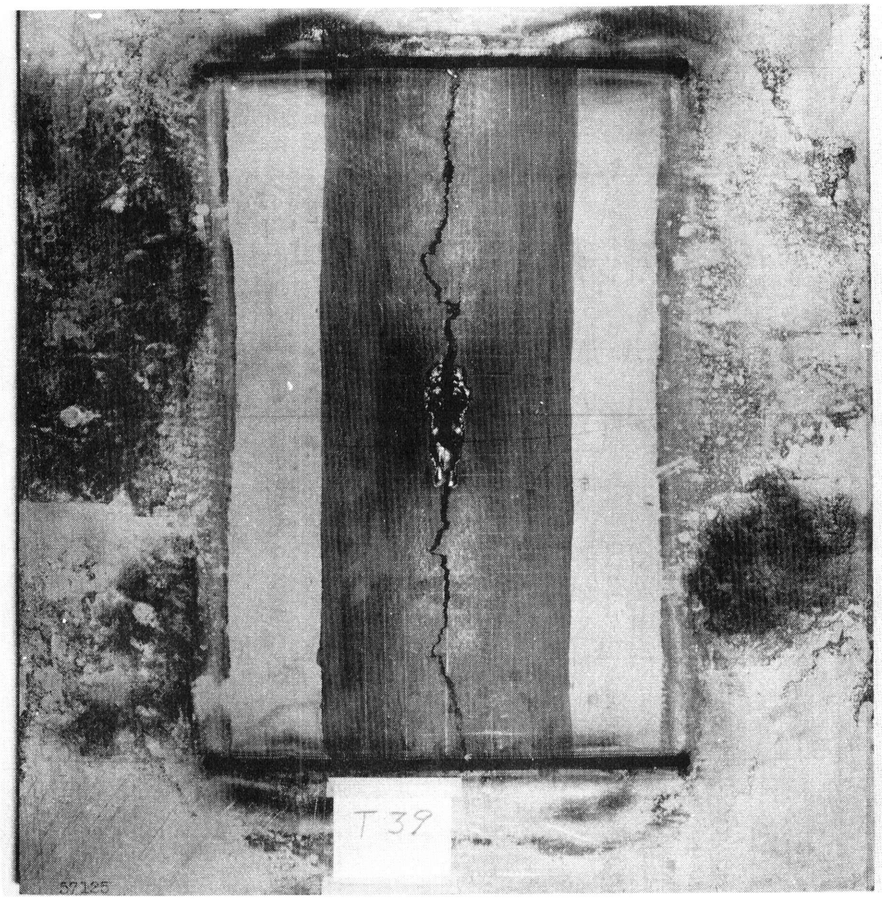

(a) top view

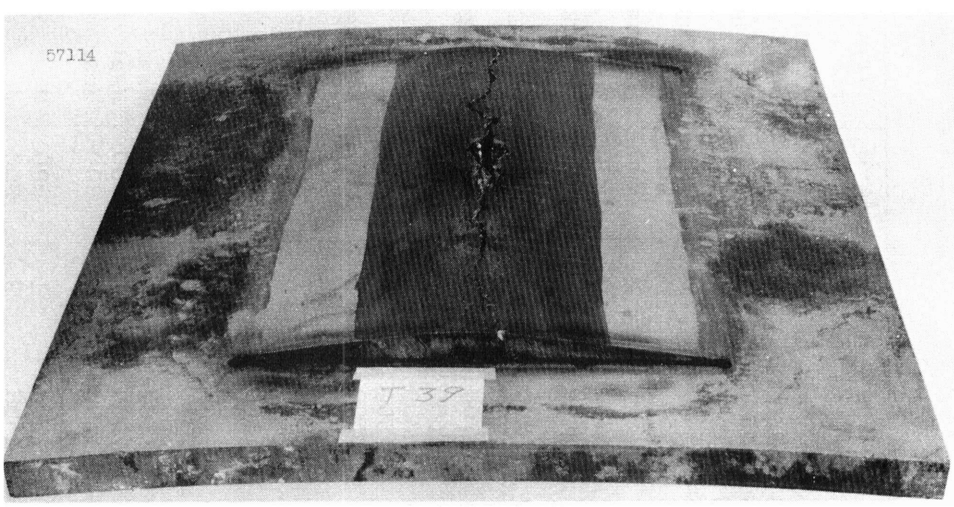

(b) end view

Fig. 1 - Explosion tear test specimen of Ti-7Al-2Cb-1Ta (T-39) explosively loaded to a 3-5 percent permanent strain deformation

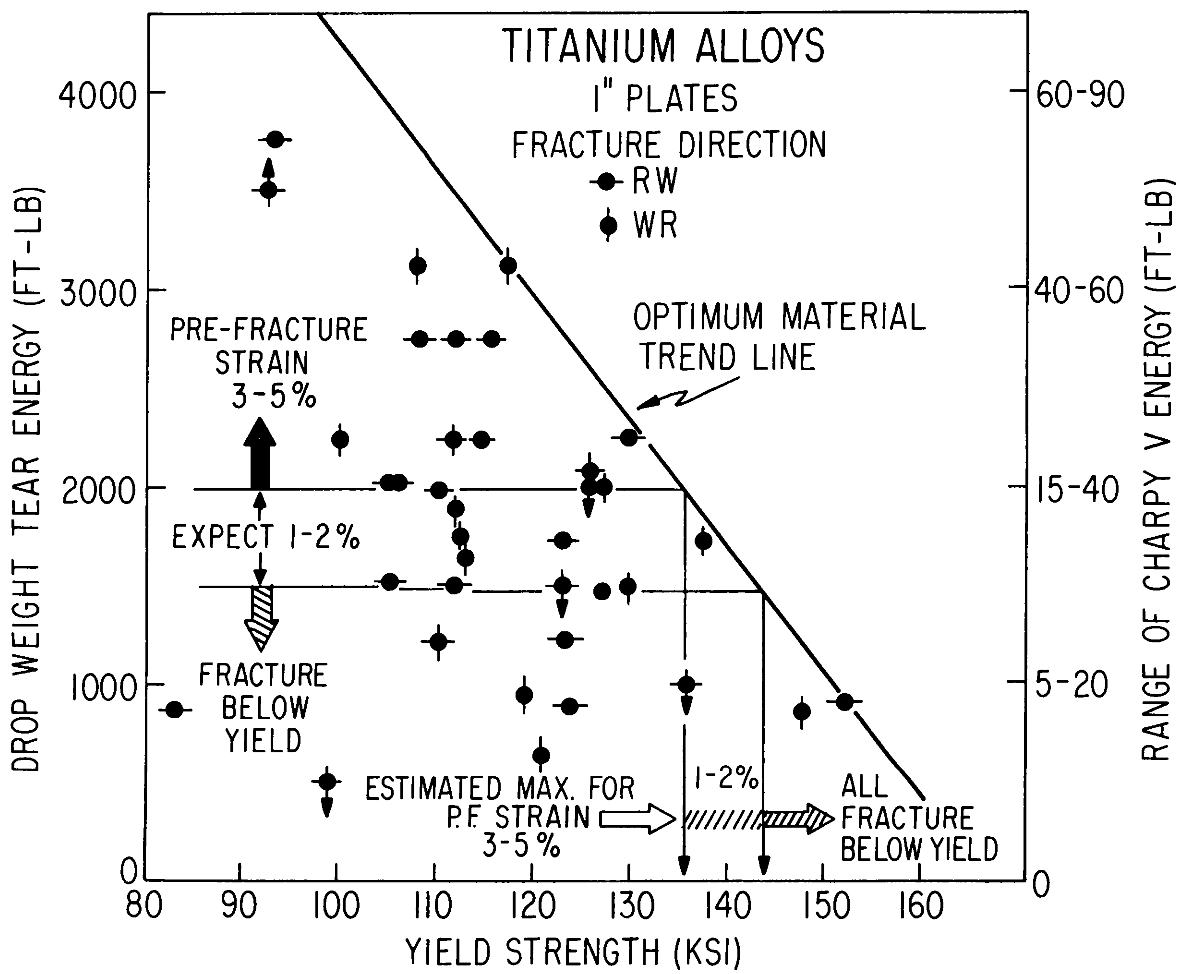

Fig. 2 - Preliminary correlation of DWTT and equivalent C_V values with ETT as a function of YS

(a) 1875°F; 1 hr in an argon atmosphere. 50X.

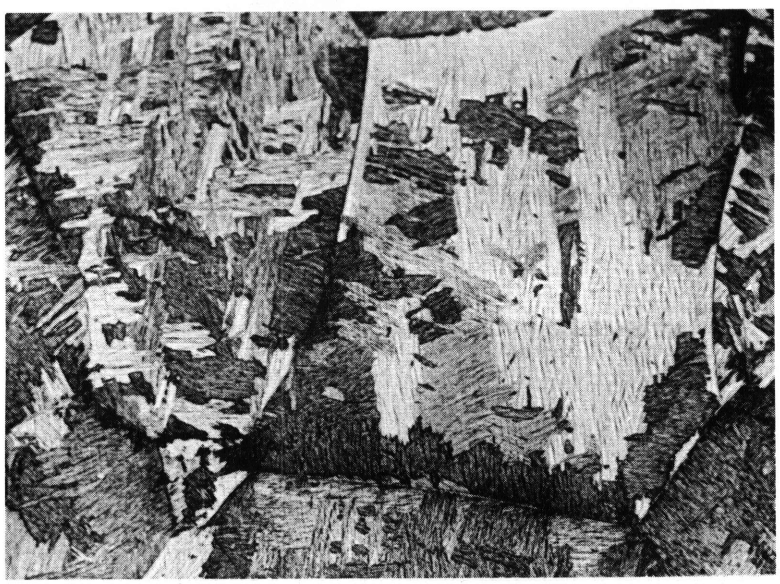

(b) 1900°F; 1 hr in an argon atmosphere. 50X.

Fig. 3 - Microstructure of commercially produced Ti-8Al-1Mo-1V alloy (T-19) heat-treated above and below the beta transus

(a) 1875°F; 1 hr in an argon atmosphere. 50X.

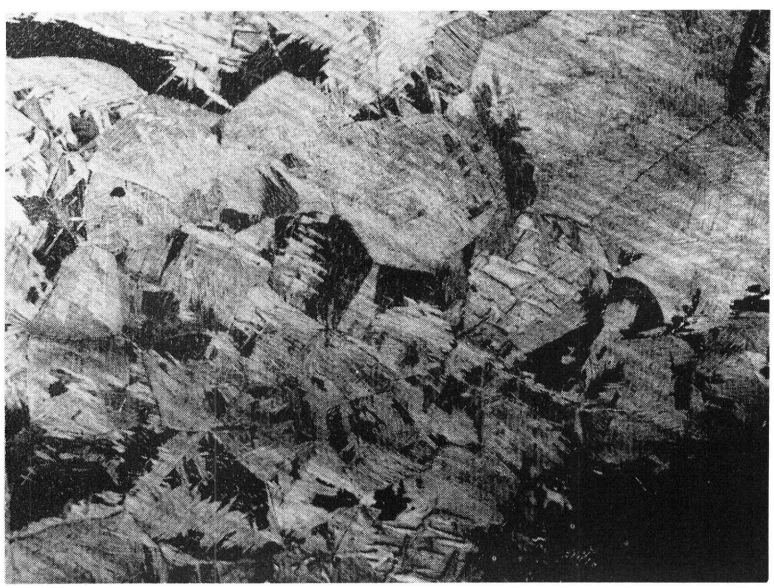

(b) 1900°F; 1 hr in an argon atmosphere. 50X.

Fig. 4 - Microstructure of NRL-produced and INFAB forged-and-rolled extra low interstitial Fi-8Al-1Mo-1V alloy (T-28) heat-treated above and below the beta transus

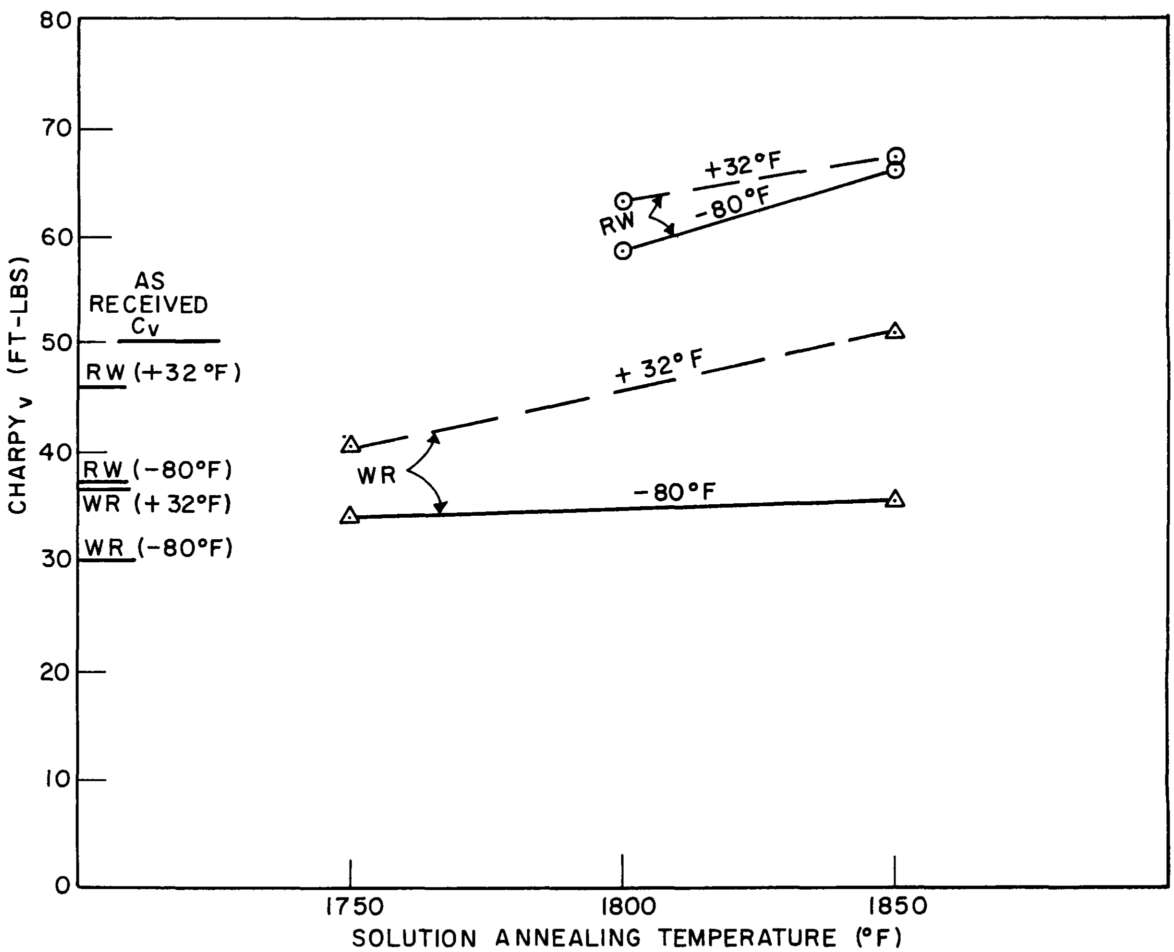

Fig. 5 - Effects of solution annealing temperature on the Charpy V-notch energy of the alloy Ti-8Al-1Mo-1V (T-28) with a common 1100°F age for 2 hr and water quenched.

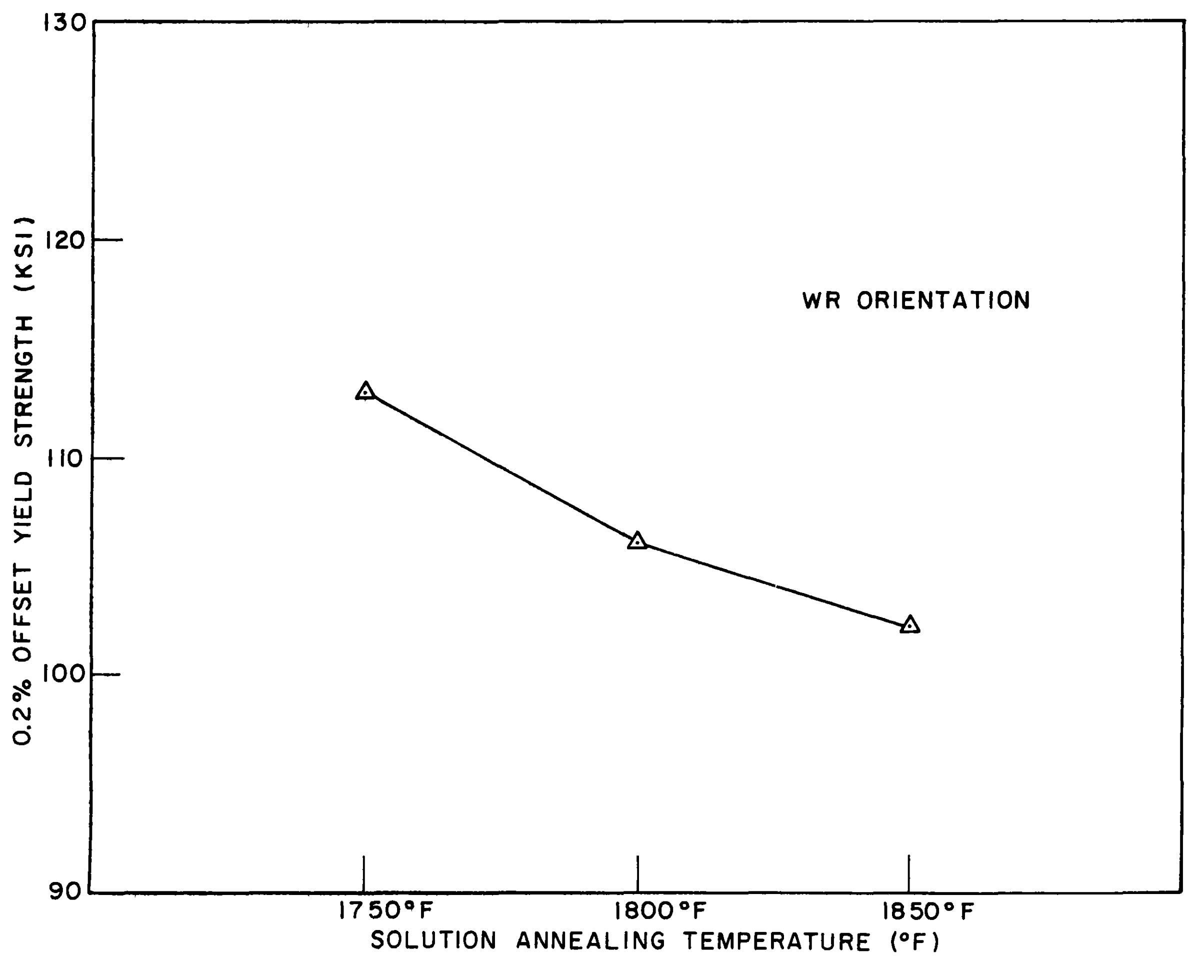

Fig. 6 - Effects of solution annealing temperature on the YS of the alloy Ti-8Al-1Mo-1V (T-28) with a common 1100°F age for 2 hr and water quenched.

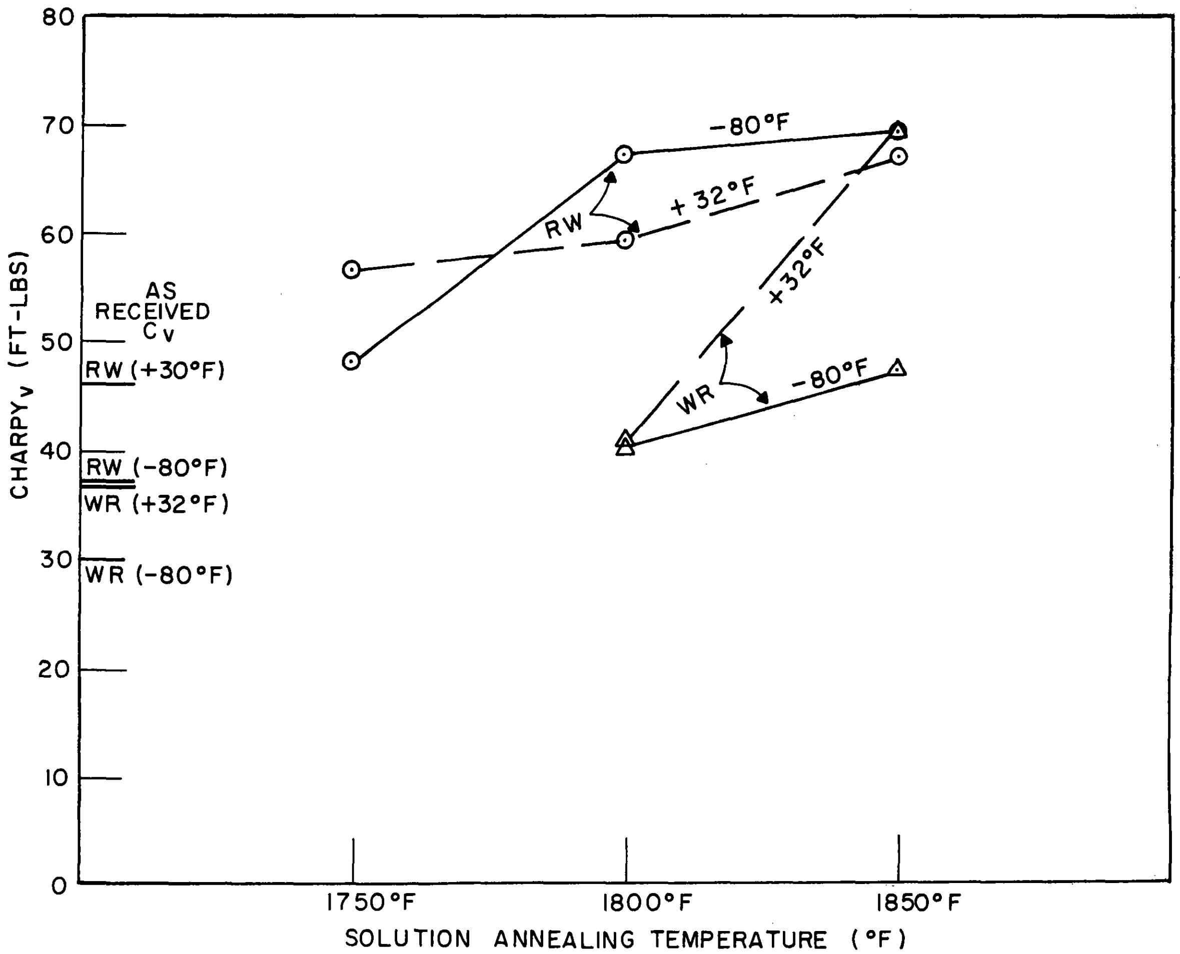

Fig. 7 - Effects of solution annealing temperature on the Charpy V-notch energy of the alloy Ti-8Al-1Mo-1V (T-28) with a common 1200°F age for 2 hr and water quenched.

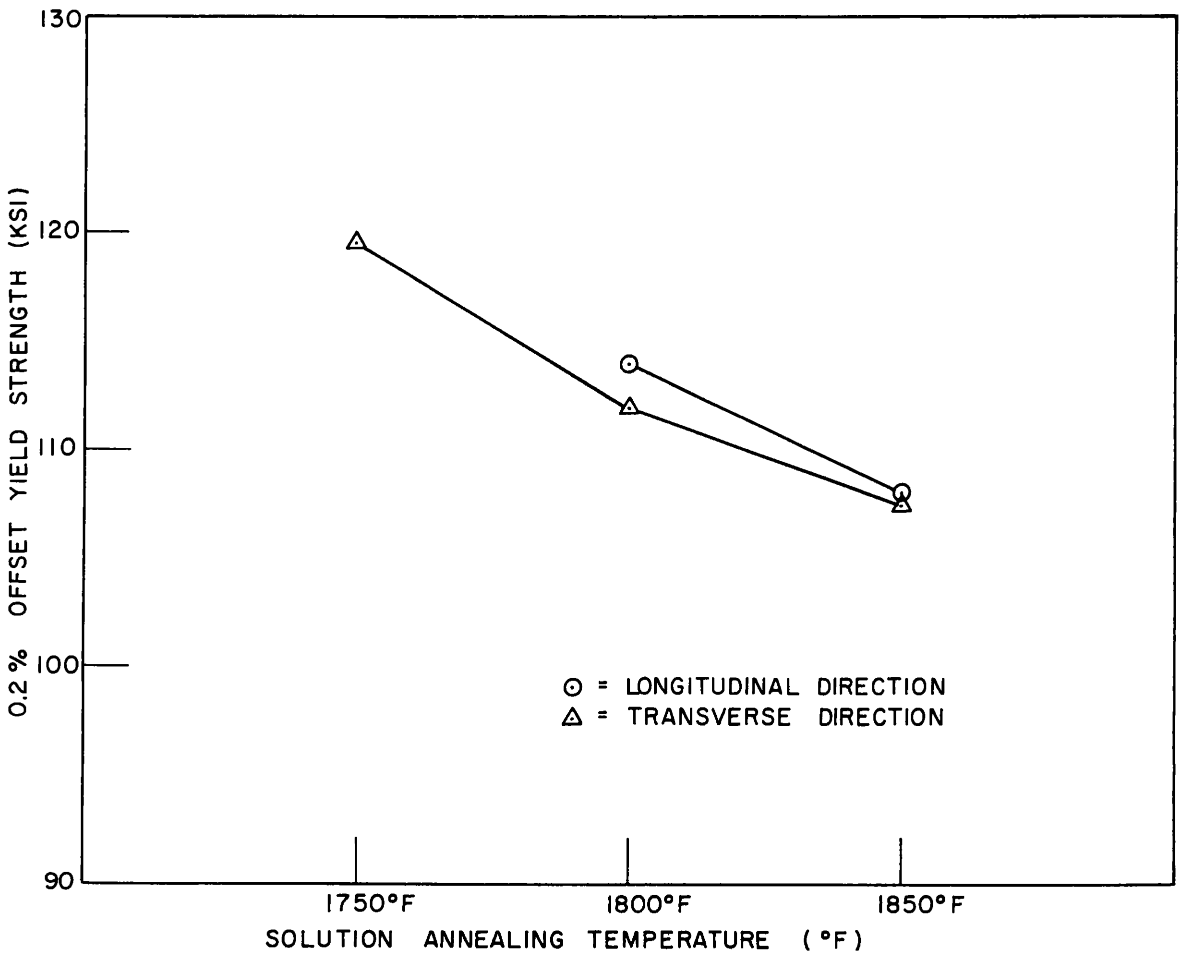

Fig. 8 - Effects of solution annealing temperature on the YS of the alloy Ti-8Al-1Mo-1V (T-28) with a common 1200°F age for 2 hr and water quenched.

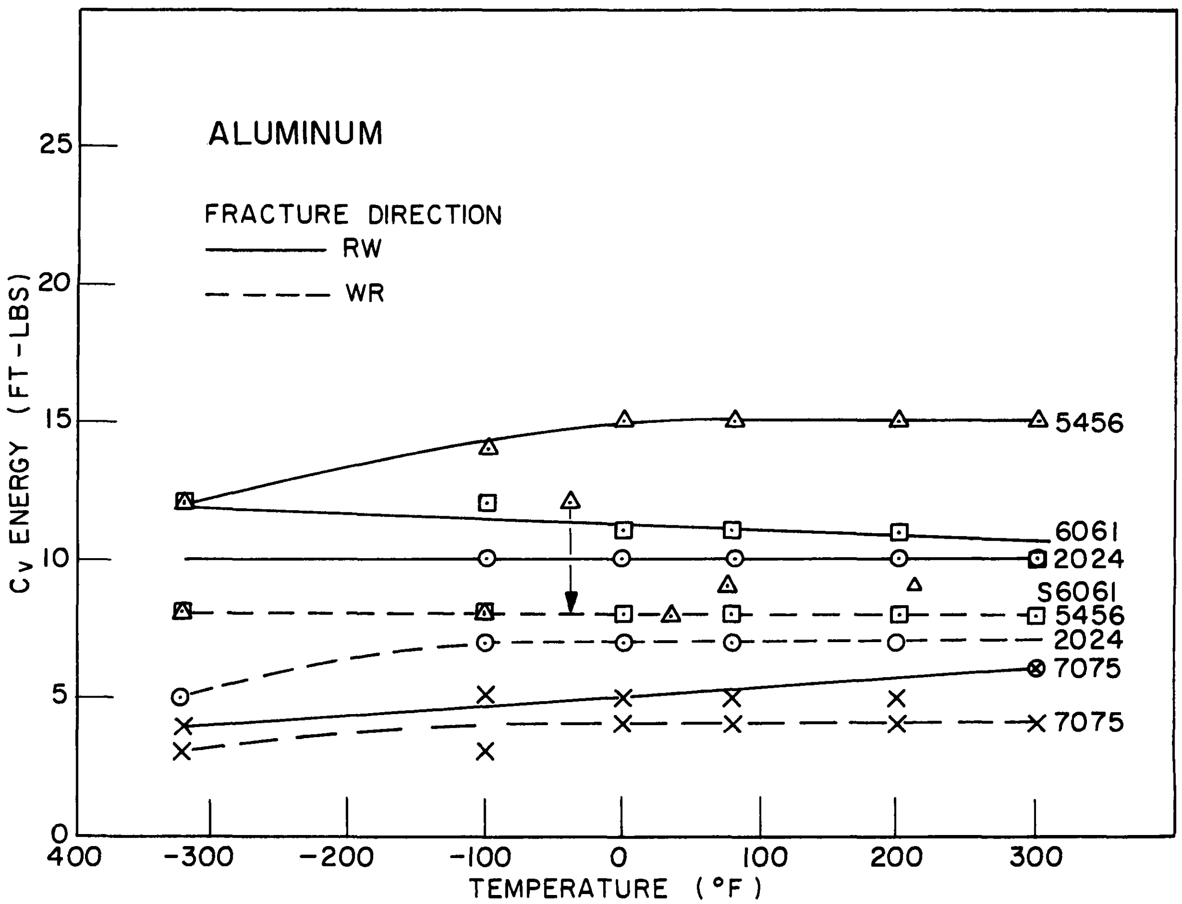

Fig. 9 - Charpy V-notch energy as a function of temperature

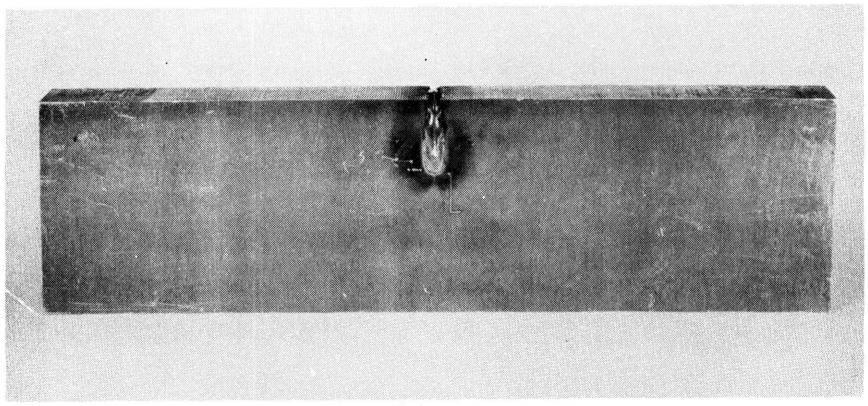

Fig. 10 - Aluminum alloy drop-weight tear specimen with electron beam crack starter weld

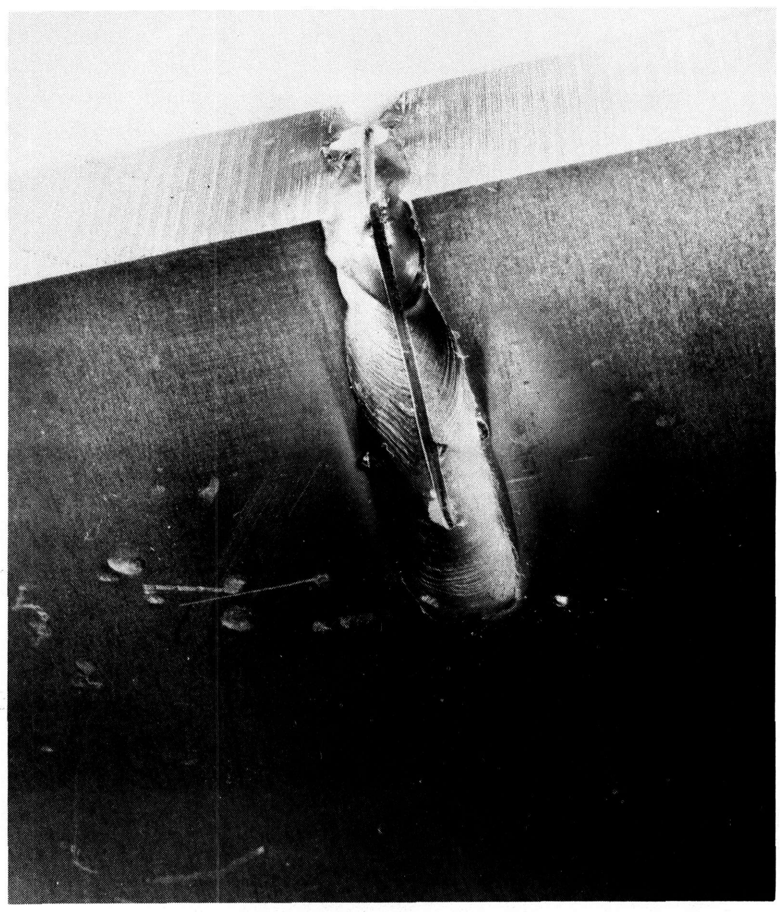

Fig. 11 - Aluminum alloy drop-weight tear specimen with electron beam crack starter weld

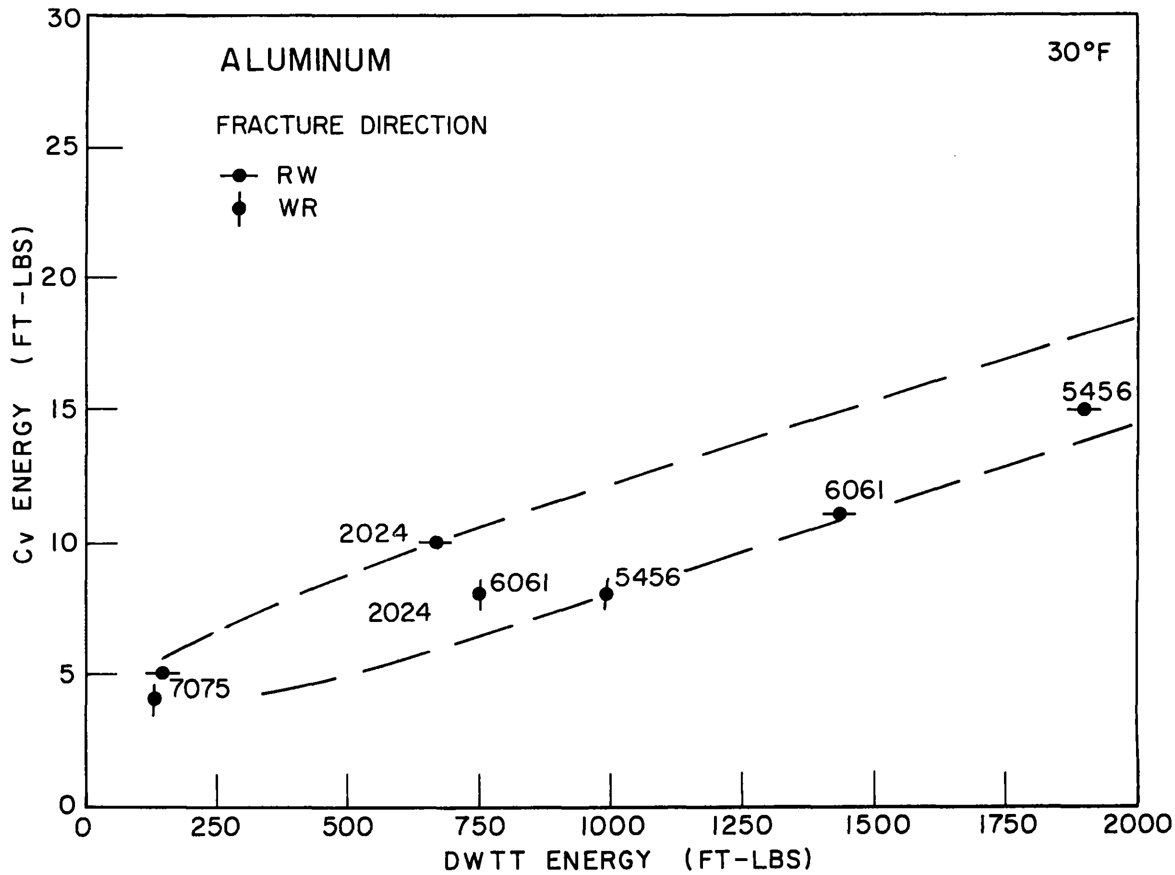

Fig. 12 - Correlation of Charpy V-notch energy with drop-weight tear energy at 30°F

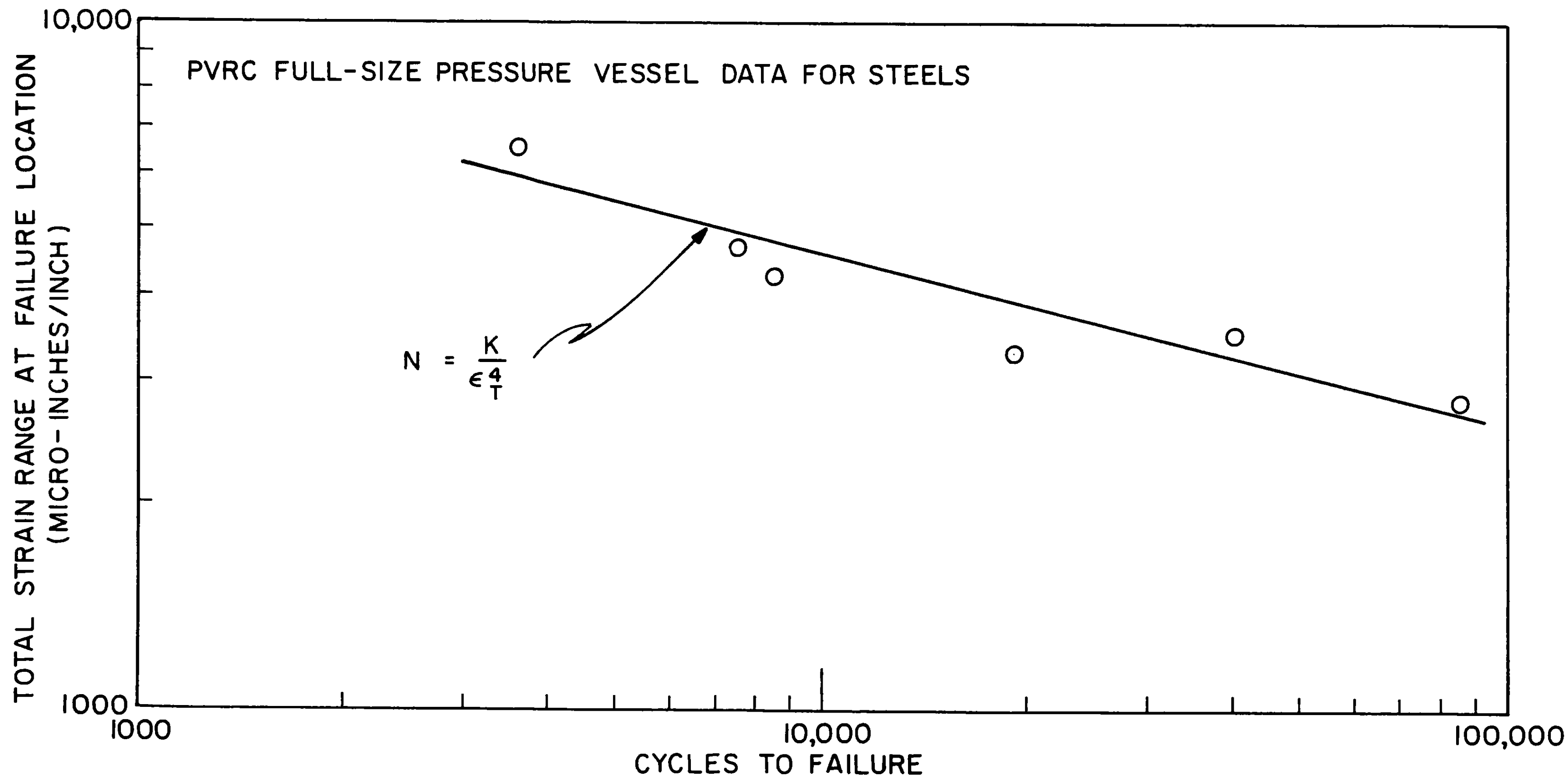

Fig. 13 - Results of low-cycle fatigue tests on full-size pressure vessels (from Ref. 5)

This page intentionally left blank.

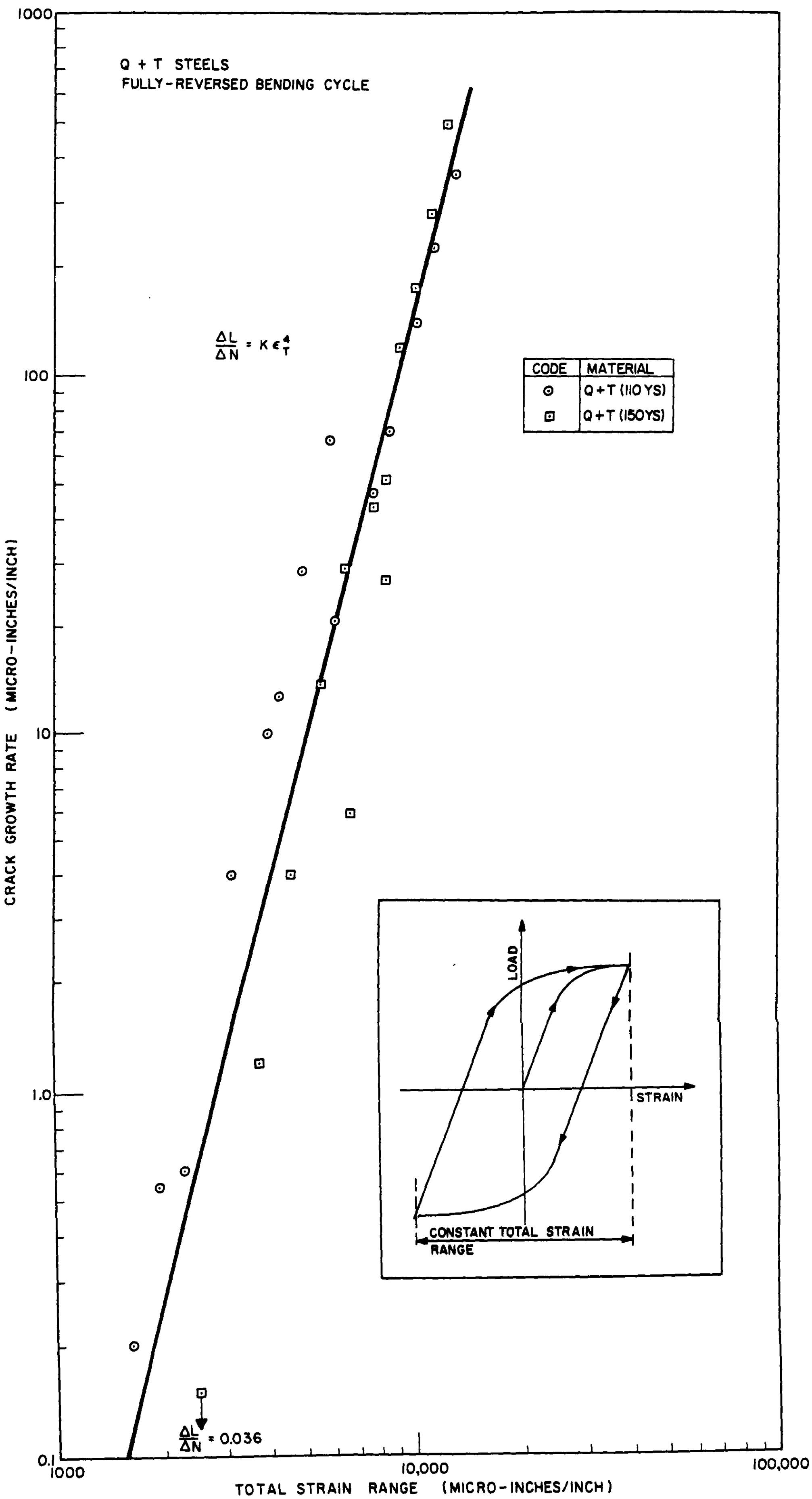

Fig. 14 - Data for crack growth rates in Q&T steels as a function of applied total strain range obtained from NRL plate-bend low-cycle fatigue tests. A diagram of the loading cycle is also shown.

This page intentionally left blank.

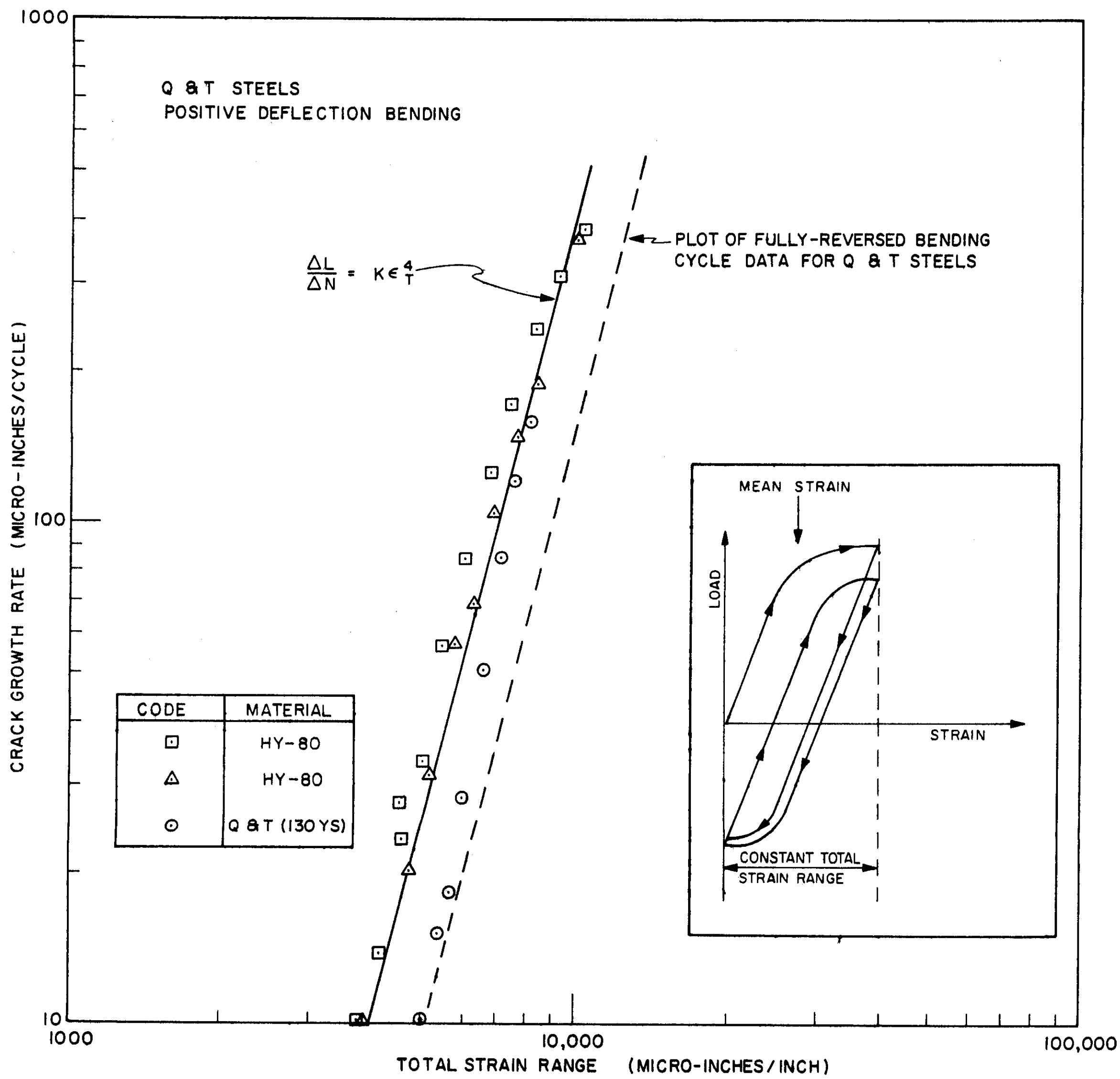

Fig. 15 - Data for crack growth rates in Q&T steels as a function of applied total strain range obtained from NRL plate-bend low-cycle fatigue tests. The effect of mean strain and a diagram of the loading cycle are shown.

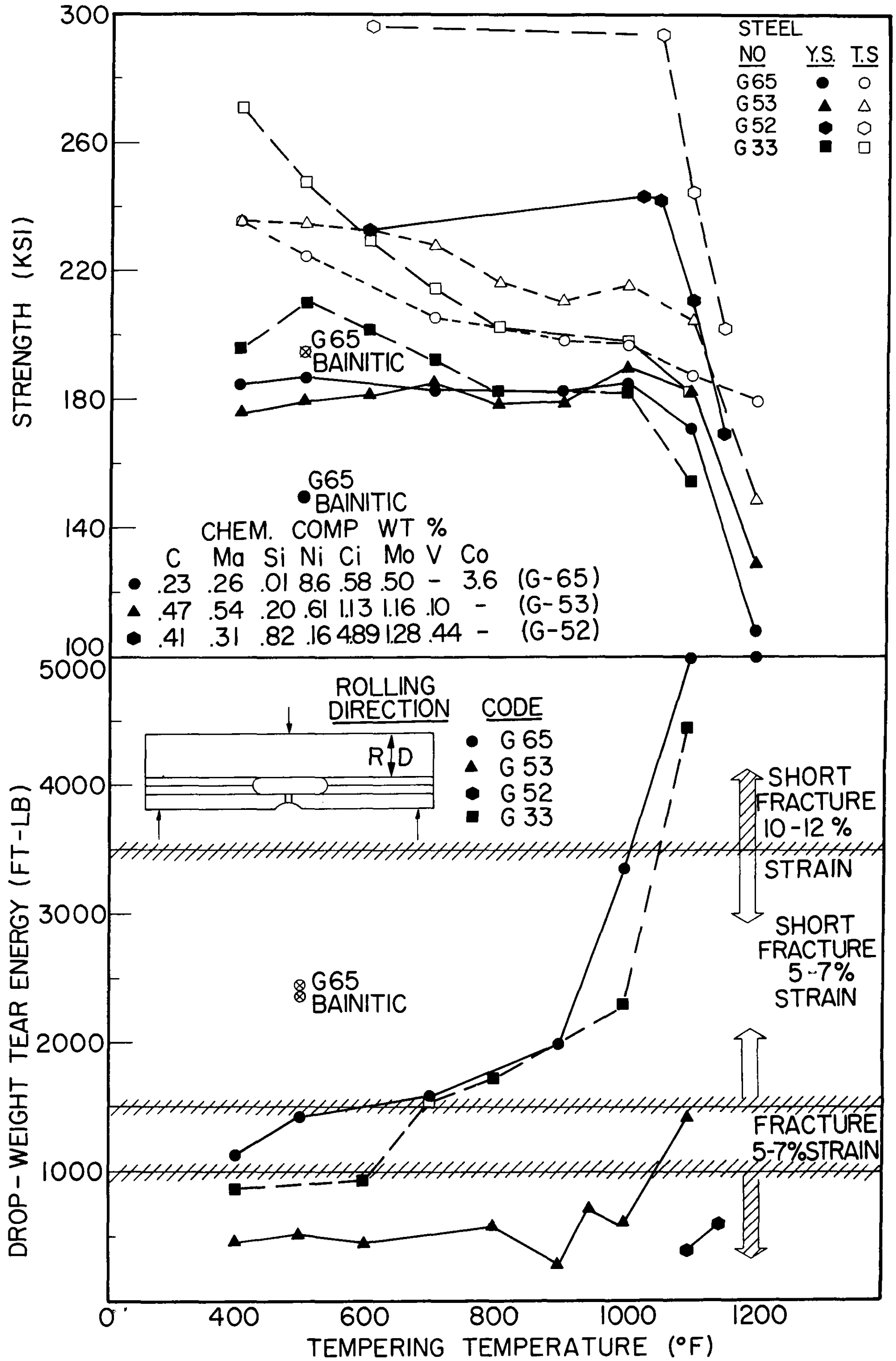

Fig. 16 - Illustrating the effects of tempering temperature on strength and drop-weight tear energy values of three proprietary high carbon content, specially processed (CEVM) steels

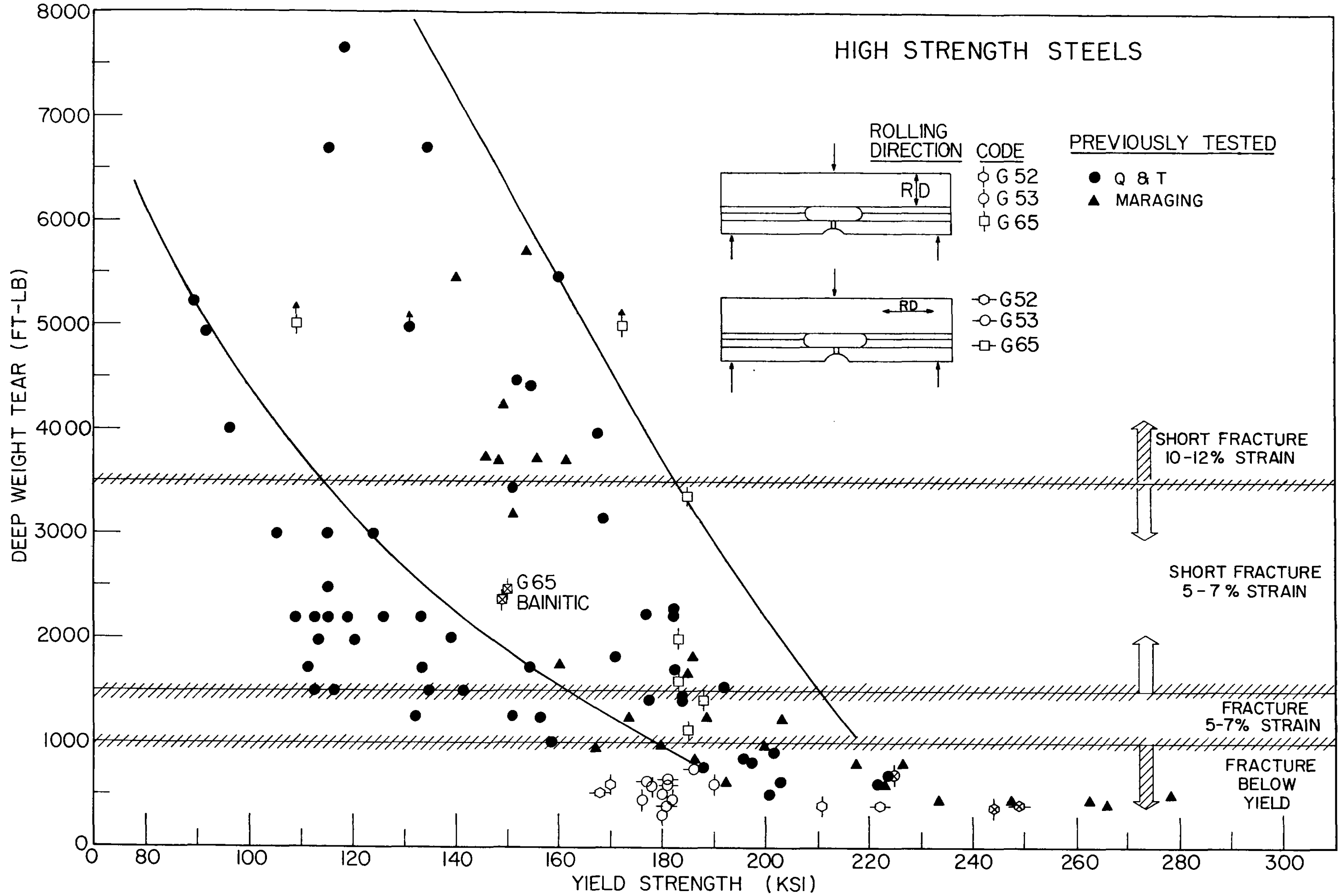

Fig. 17 - Comparison of drop-weight tear and yield strength relationships for the high carbon content proprietary steels with those of previously tested steels. The correlations with performance in the explosion tear test in the presence of 2-in. flaws are indicated by crosshatched lines and the legend at the lower right side of the illustration.

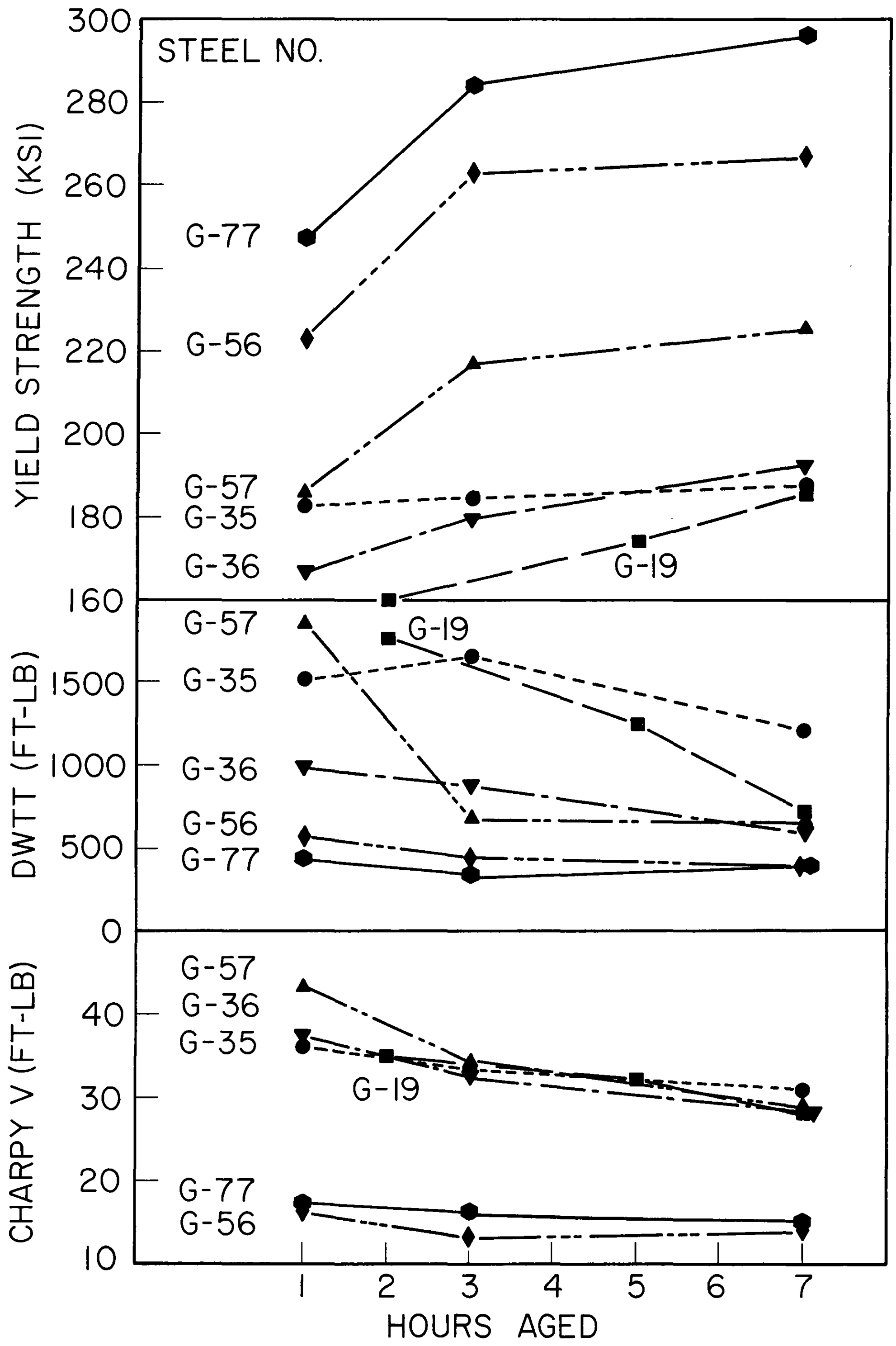

Fig. 18 - Illustrating the effects of increasing aging times on strength, drop-weight tear, and Charpy V energy values of five 18 percent Ni-Co-Mo and one 12 percent Ni-Cr-Mo maraging steels

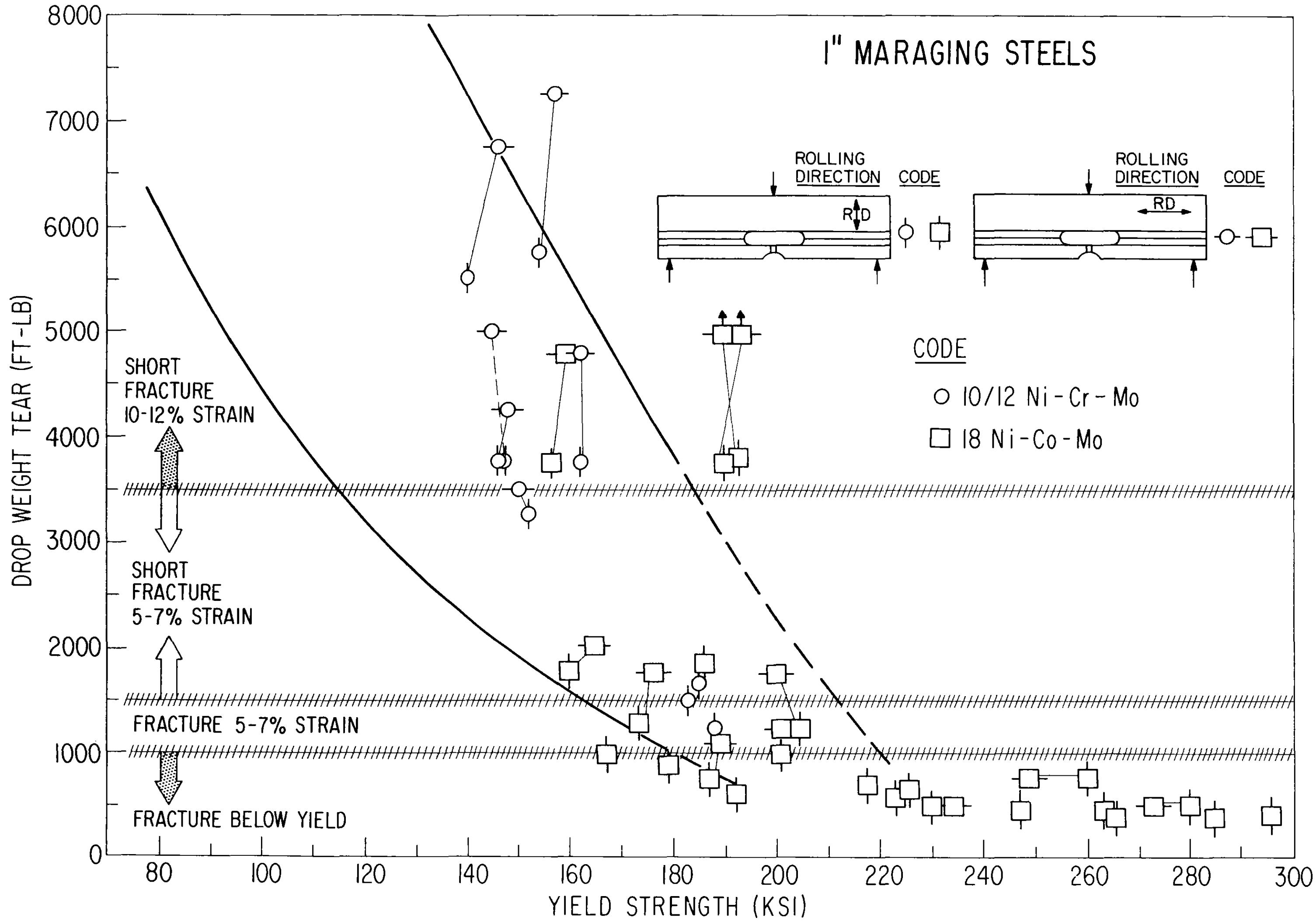

Fig. 19 - Summary of drop-weight tear and yield strength relationships for maraging steels. The correlations with performance in the explosion tear test in the presence of 2-in. flaws are indicated by the crosshatched lines and the legend at the left side of the illustration.

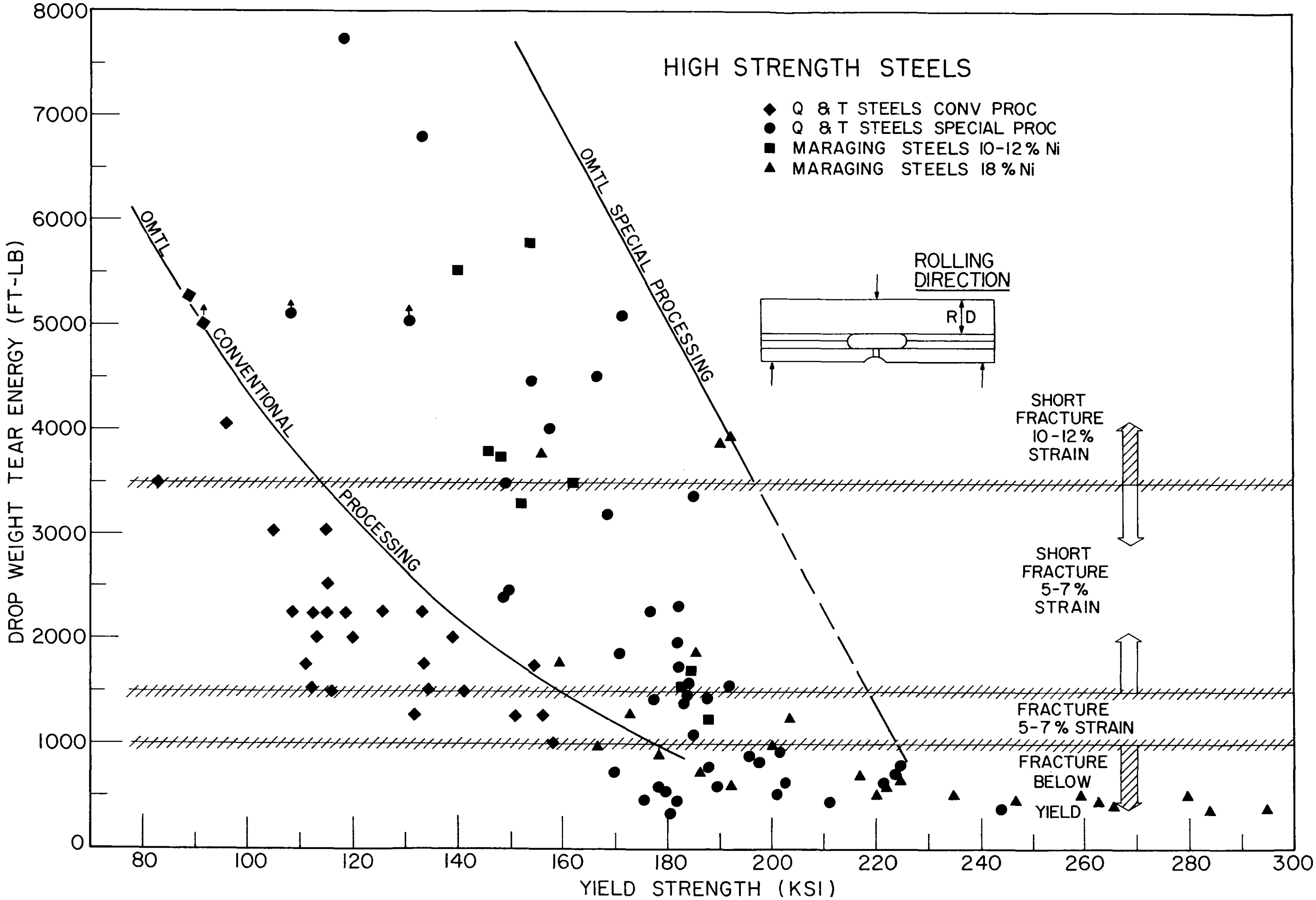

Fig. 20 - Summary of drop-weight tear and yield strength relationships for all steels tested to date. The correlations with performance in the explosion tear test in the presence of 2-in. flaws are indicated by the crosshatched lines and the legend at the lower right side of the illustration.